THE ABSORPTION OF NITROGEN DIOXIDE BY CONDENSING WATER DROPLETS

A THESIS

Presented To

The Faculty of the Division of Graduate Studies and Research

by

John Patrick Herrmann

In Partial Fulfillment

of the Requirements for the Degree

Master of Science in Chemical Engineering

Georgia Institute of Technology

December, 1977

THE ABSORPTION OF NITROGEN DIOXIDE

BY CONDENSING WATER DROPLETS

Approved:

Michael J. Matteson, Chairman

Edwin M. Hartley

Charles W. Gorton

Date approved by Chairman 11/14/77

If a man will begin with certainties, he shall end in doubt, but if he will be content to begin with doubt, he shall end in certainties . . . This is the foundation of all: for we are not to imagine or suppose, but to discover, what nature does, or may be made to do.

from The Advancement of Learning

Francis Bacon
Viscount, St. Albans
1561 - 1626

ACKNOWLEDGMENTS

The author is grateful for the assistance which was received during the course of this study. Dr. M. J. Matteson, Chairman of the Thesis Committee, provided not only his technical expertise during this work but also provided his confidence and friendship which made completion of this work possible. The author also thanks the members of the Reading Committee, Drs. E. M. Hartley and C. W. Gorton, for their comments, and other members of the faculty for technical advice when sought. In particular, he wishes to thank Dr. R. S. Roberts for providing his support both academically and socially.

The author appreciates the support rendered by his family, both spiritually and monetarily, during his extended stay at Georgia Tech. Likewise, he wishes to thank his close friends, and in particular Michael Mullins, who provided a source of comfort during this period of this work.

TABLE OF CONTENTS

LIST OF TABLES

LIST OF ILLUSTRATIONS

LIST OF ILLUSTRATIONS (Continued)

SUMMARY

An investigation was undertaken to observe the absorption of nitrogen dioxide in ambient concentrations of 100 and 300 parts per million (ppm) in humid air streams with dew points of 19.5°C, 15.5°C, and 11.5°C, and 5.5°C by a liquid drop with an initial temperature of 5.0°C, at exposure times of 0, 5, 10, 15, 20, 25, 30 and 60 seccnds. The results indicate that under optimum conditions for condensation, 102% and 52.3% greater absorption occurs than would be expected by the Henry's law equilibrium value for the 100 and 300 ppm cases, respectively.

The amount of NO_2 absorbed varied linearly with the amount of water condensed, and it can be seen qualitatively that absorption continues to occur while condensation is occuring. This phenomenon can be explained by the theory of continuous surface renewal, thus exposing new sites for absorption, in addition to Stefan flow.

CHAPTER I

INTRODUCTION

The absorption of a gas by a liquid is a basic chemical engineering unit operation which has been well studied. When it is desired to form a product, as in the case of nitrogen dioxide absorption by water to form nitric acid, or to clean an effluent gas stream of a particular pollutant, the unit operation is commonly referred to as "scrubbing."

Investigation of physical parameters, such as composition, contact time, and solubility have been published in large amounts. Recently, techniques which affect surface characteristics of the liquid, and particularly a liquid droplet, such as surfactant (42) and surface charge (16) have been made.

Another method for altering the surface characteristics of a drop is surface renewal by condensation, and, conversely, surface deterioration by evaporation. Bagaevskii (3) showed that gas absorption is enhanced during condensation as compared with a drop with a stagnant surface layer.

In work previously performed at the Georgia Institute of Technology, Wills (46) and Oliver (31) have shown that absorption of sulfur dioxide (SO_2) and oxygen (O_2) was enhanced during condensation of a humid gas mixture on a cold water droplet. Since nitrogen dioxide (NO_2) is often present in the atmosphere as a result of combustion processes, it is likely that this gas often becomes "trapped" in water droplets via the same mechanism as discussed above.

Therefore, nitrogen dioxide (NO_2) in the range of 100 to 300 parts per million (ppm) was used as the gas for this investigation. As NO_2 is a primary species in the photochemical oxidation of the atmosphere commonly referred to as smog, it represents a serious pollution problem, and it would be of significant importance to develop or enhance methods for its elimination. Therefore, the study of nitrogen dioxide during a period of condensation on a water droplet is a justifiable extention of work previously performed in the field of gas absorption.

CHAPTER II

GENERAL DISCUSSION AND LITERATURE PREVIEW

General Theory

The absorption of one component of a gas phase mixture by a liquid droplet is actually a complex set of individual steps. These include: (1) diffusion from the gas phase to the surface of the droplet, (2) adsorption on the droplet followed by the surface chemical reaction, if any, (3) absorption into the droplet accompanied by chemical reaction, if any, and (4) desorption of the unused reactants and products.

Due to the complexity of the system, certain simplifing assumptions have been made in the classical theoretical development and description of gas absorption models. Three theories have been introduced: the film theory, the penetration theory, and the boundary layer theory.

The film theory assumes steady state, and visualizes a "stagnant film" in each phase which constitutes the resistance to mass transfer. Other assumptions include complete mixing in both bulk phases and chemical equilibrium at the interface. Clearly, as Danckwerts (10) maintains, the film theory is too simple and unrealistic.

The penetration theory, proposed by Higbie (21) does not assume steady state. In his development Higbie integrated Fick's Second Law of Diffusion. *

* Symbols are defined in Appendix A.

$$\frac{dD_A}{dt} = D_A \frac{d^2C_A}{dx}$$

to give:

$$NA = [C_{AX} - C_{AOL}] \left[\frac{\overline{[D_A]}}{t}\right]^{1/2}$$

Since equilibrim is never reached at the interface, the penetration theory is only applicable when the diffusing molecules have not completely penetrated the fluid layer, which implies short exposure times. The penetration theory has been found particularly useful in defining the mass transfer into a falling liquid film in the presence of a gas.

The most recent of the three theories is the boundary layer theory. It presents a two dimensional velocity profile discussion for mass transfer at the interface. If one of the velocity profiles is zero, as in the case of a solid in contact with a liquid, the boundary layer next to the interface must be laminar. In addition, for the turbulent region, the following approximation for the mass transfer coefficient has been presented by Bird (5), et. al.:

$$Sh = 2.0 + 0.6\ Re^{1/2}\ Sc^{1/3}$$

However, Angelo (2) has shown that for periods of continuous surface renewal, the observed mass transfer may be fifteen times as large as that predicted by boundary layer theory. Therefore, the unsteady state

absorption during surface renewal is a complex situation which is not directly applicable to any of the theories generally accepted.

Absorption by Droplets

Due to the unique surface tension characteristics of a liquid droplet, the theories which have been previously mentioned are not directly applicable as they imply a bulk phase with rising gas bubbles or a wetted wall column. Several investigations have shown the effects of interfacial velocity, drop diameter, diffusivity, and concentration of a dilute gas absorbed by a quiescent water drop. Johnstone and Williams (22) worked with ammonia, hydrogen chloride, sulfur dioxide, hydrogen sulfide and carbon dioxide and confirmed the rate of absorption theory proposed by Johnson and Kleinshmidt (21):

$$\frac{dN}{d\Theta} = AKg \sqrt{\frac{P}{P_{BM}}} [P_{A1} - P_{A2}]$$

where the gas film coefficient for a quicescent drop is:

$$Kg = \frac{1}{1.5RT} \sqrt{\frac{b}{D_s}} [2\ g\ L]^{0.25}$$

and for a moving drop:

$$Kg = \frac{1}{1.5RT} \sqrt{\frac{b}{D_s}} \left| \frac{\overline{Vg} + \sqrt{2\ g\ L}^{3/2} - \overline{Vg}^{3/2}}{\sqrt{2\ g\ L}} \right|$$

Whitman, Long, and Wang, (45) who pioneered the theory of absorption by liquid drops, showed that the rate coefficients of absorption were enhanced by the surface effects of the drop over bulk phase absorption theories. Also, they showed that absorption during the period of drop formation showed even a more significant increase in the absorption of a soluble gas by the liquid droplet.

Other workers have extended this work. Angelo (2) developed the surface stretch model of surface renewal. Groothius and Kramers (20) and Beek and Kramers (26) developed a model which predicts mass transfer coefficient based on continuous formation of fresh surface during droplet growth. Rajan and Heideger (37) have discounted this approach as it does not incorporate the critical parameter of internal circulation. Dixon and Russell (13) have hypothesized that enhanced absorption during droplet formation is due to turbulence during formation.

For very dilute solutions of water [10^{-3} to 10^{-5}] surface tension characteristics observed by Jones and Ray (23) indicated that absorption of ions at the surface continues until a number of sites, typically 5 sites per 10^{5} surface molecules, have been occupied. For a typical aerosol in which the droplets are smaller than five microns [μm] in diameter, ordinary mass transfer mechanisms are not directly applicable. Therefore, at least to some extent, the uptake of a gas at the surface of a water droplet is a surface phenomenon. Consequently, if the surface is continuously renewed, as in drop formation or condensation, one would expect the number of available sites to continue to increase in each successive "shell" of water. Another possible mechanism for the enhancement of adsorption during surface renewal is Stefan flow, in which gas molecules

are physically trapped by the surface renewal sequence.

Nitrogen Dioxide Absorption

Despite the extremely poisonous nature of nitrogen dioxide (200 ppm exposure is considered lethal according to the Merck Index) a voluminous amount of research has been done concerning nitrogen dioxide [NO_2] absorption in water. This particular scrubbing operation is extremely important in the production of nitric acid and, therefore, its equilibrim reactions are well documented. However, in large concentration (1%) the NO_2 species actually occurs in its dimmer form, namely dinitrogen tetroxide [N_2O_4]. The dynamic equilibrium of the two species

$$2NO_2 \rightleftharpoons N_2O_4 \qquad (1)$$

can be represented by

$$K_1 = \frac{[N_2O_4]^{1/2}}{[NO_2]}$$

Typical values of K_1 are: @ 0^oC, $K_1 = 8.060$; @ 18.8^oC, $K_1 = 3.710$ (30).

For absorption in water at concentration typical of nitric acid manufacture, the following sequence of reactions have been proposed:

$$2NO_2\ [N_2O_4] + H_2O \rightleftharpoons HNO_2 + HNO_3 \qquad (2)$$

$$2HNO_2 \rightleftharpoons NO + NO_2 + H_2O \qquad (3)$$

thus yielding the over-all reaction

$$3NO_2 + H_2O \rightleftharpoons NO + 2HNO_3 \qquad (4)$$

Where the equilibrium constant, K_4 is represented by

$$K_4 = \frac{(NO)\ (HNO_3)^2}{(NO_2)^3\ (H_2O)}$$

at 25°C, $K_4 = 0.137\ atm^{-1}$ (30).

In the reaction sequence, step (2) is considered the rate determining step with the rate of formation of nitric acid given by:

$$R_{HNO_3} = k_f\ (NO_2)^2\ (H_2O) - k_f'\ (HNO_2)\ (HNO_3)$$

with rate constants given by:

$$k_f = 5.5 \times 10^4\ l^2\ mol^{-2}\ sec^{-1}$$

and

$$k_f' = 5.85\ l\ mol^{-1}\ sec^{-1}$$

at 25°C (14).

The equilibrium constant for the above reaction is given by:

$$K_2 = \frac{[HNO_2]^2}{[NO_2]\ [NO]\ [H_2O]}$$

with a typical value of $K_2 = 1.5\ atm^{-1}$ (14) at 25°C. The sequence of reactions therefore indicates that the reaction between water and dinitrogen tetroxide is first order in N_2O_4 and, thereby, is second order in nitrogen dioxide.

There is considerable dispute as to the actual rate determining step during the absorption of the NO_2-N_2O_4 mixture by the water drop. Chambers and Sherwood (41) have proposed a "two film" theory in which the gas film is rate controlling. Denbigh and Caudel (7) showed that by increasing the bulk liquid volume in the wetted wall column, no effect was realized on the rate of removal of nitrogen oxides by water, thus indicating the importance of the interfacial area between the gas and the liquid. Later, Denbigh and Prince (12) showed that the absorption rate was controlled by the chemical reaction in the liquid phase. However, Peters (34) et. al. concluded that the chemical reaction in the gas phase was the controlling mechanism for absorption.

Dekker, (11) et. al. concluded that only the N_2O_4 species took part in the formation of nitric acid which, therefore, emphasizes the significant feature of the discussion up to this point.

All of the investigators cited thus far have worked with extremely high concentration (3% to 68% by volume NO_2 - N_2O_4). As previously mentioned, high concentration shift the NO_2 - N_2O_4 equilibrium toward the

latter.

Work at low concentration, i.e., the parts per million range of nitrogen dioxide absorbed into water, are relatively few. Borok (6) determined the Henry's law constant for solubility of NO_2 in bulk phase water to be H = 100 atm.

Other investigators, such as Palmers (32) et. al. and Crecelius and Forwerg (9) agree with Dekker in that reaction (2) above does not proceed to any significant extent at low pressure and low concentration of NO_2. Instead, they picture a mechanism in which NO_2 proceeds to NO_2^- ion in the presence of a water droplet via the following mechanism:

$$3NO_2 + H_2O \rightleftarrows NO + 2HNO_3 \qquad (5)$$

$$H_2O + HNO_3\ 2NO \rightleftarrows 3HNO_2 \qquad (6)$$

$$HNO_2 \rightleftarrows H^+ + NO_2^- \qquad (7)$$

The relationship between the formation of nitrogen dioxide ion and the molecular nitrogen dioxide has been shown by Crecelius (9) to be a function of concentration. At 1.0 ppm, the ratio of NO_2^-/NO_3^- is 99/1 whereas at 1000 ppm the ratio is 50/50. For the purpose of this work the ratio was assumed to be a constant value of 1.7 moles of NO_2 per mole of NO_2^-, and thereby agrees with the 0.57 equivalency factor mentioned in the testing procedure, which will be discussed later.

Because of tremendous gap in research at the low concentration range, this research was undertaken. Previously, work at the Georgia

Institute of Technology by Wills (46) and Oliver (31) have shown increased total absorption of sulfur dioxide and oxygen during water condensation above the saturation value expected by Henry's law. Therefore, the purpose of this investigation was to prove whether the same trend could be extended to a gaseous species of limited hydrolizability at a pressure and concentration of fundamental importance in the abatement of NO_2 atmospheric pollution.

CHAPTER III

INSTRUMENTATION AND EQUIPMENT

In the design of any experiment, it is necessary to decide which variables are to be kept constant and which are to be varied so that a maximum of information can be obtained. Therefore, the necessary monitoring equipment must be used so that constants can be continually checked. The other part of the design in an experiment is the method in which analysis will be made after an experimental test.

The variables which were changed during the experiment were (1) concentration of NO_2 in the humid air stream, (2) the humidity of the carrier air stream, and (3) the exposure, or contact time, of the drop to the humid gas mixture. The variables which were held constant were (1) the gas flow rate through the apparatus, with a linear velocity of 50 cm/sec past the drop, (2) the temperature of the incoming NO_2- air stream at 25°C, (3) the initial drop temperature at 5°C, and (4) the initial diameter of the droplet at 0.25 cm. Atmospheric pressure remained approximately constant at 740 mm Hg.

Equipment

The flow scheme for the gas delivery system is shown in Figure 1. The air stream was regulated through the humidifying column which was kept at a constant temperature by a Haake, Model FK2, constant temperature bath. Matheson rotameters, types 6-15A and 605 were used after calibration. The humidity of the total stream was monitored by a Cambridge Model 990 hygro-

meter. The NO_2 concentration was monitored using a Beckman Model 255A ultraviolet analyzer which was calibrated by the vendor. The NO_2- humid air mixture was then sent to the solenoid valve, which when activated permitted the stream to flow into the contact chamber. It should be noted that Figure 1 is merely a schematic diagram. The actual apparatus was more complex as it was necessary to avoid moisture in the ultraviolet analyzer and avoid NO_2 in the dew point hygrometer.

The contact chamber consisted of a glass tube 60 cm in length and 3.5 cm in diameter. It was a straight tube with one main sampling station approximately 40 cm from the entrance. At the entrance of the tube was a set of baffles to insure complete mixing. Immediately above the sample port was a 26 gauge hypodermic needle which admitted a distilled, deionized 5.0°C water drop to the chamber from the ice bath, and a second 26 gauge hypodermic needle to which a thermistor had been installed so that the initial drop temperature and the temperature profile during exposure could be monitored. The thermistor was connected to a YSI model 43TD metering device, and this, in turn, was connected to a Sargent Model MR recorder. Thus, the drop was suspended between the two needles, and as this distance was held constant, the "diameter" of the elongated droplet could be monitored. Other features of the contact chamber include two drains for removing condensate and the ends which were rubber-stoppered with tubing installed to allow the air stream to enter and exit the chamber and prevent back pressure in the system. The chamber was designed and constructed at the Georgia Tech glass blowing laboratory.

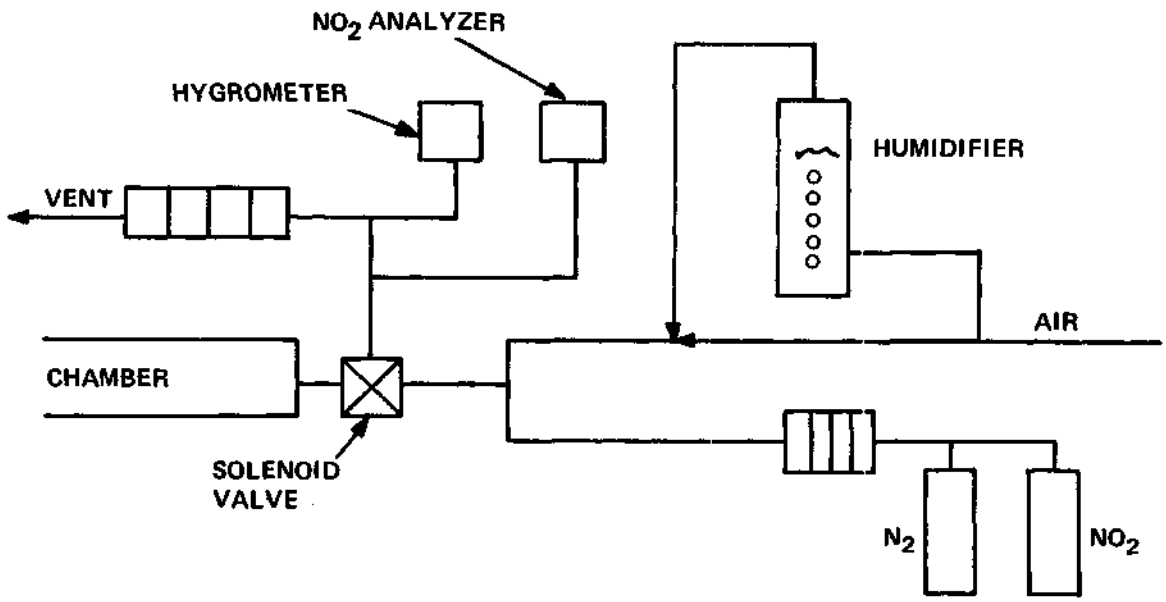

Figure 1. Schematic of Apparatus

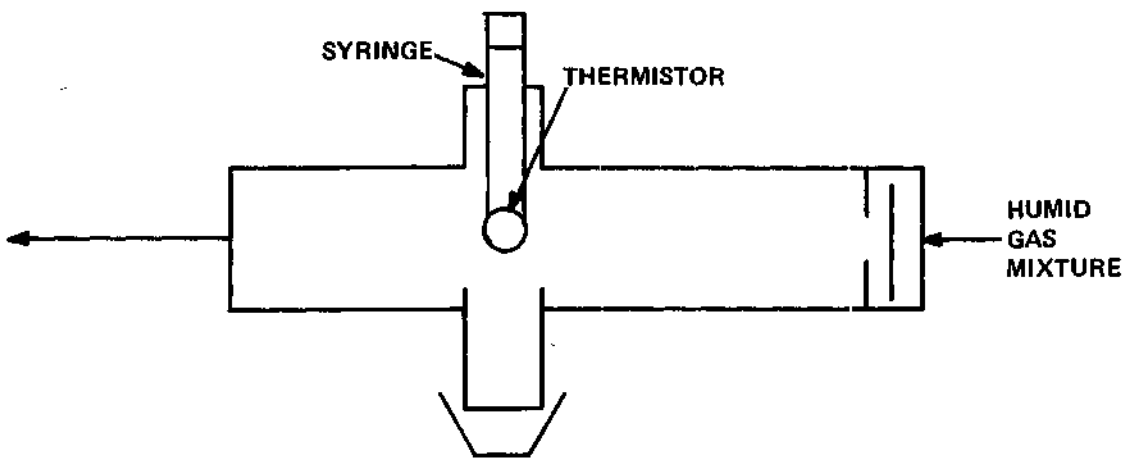

Figure 2. Schematic of Contact Chamber

Analytical Methods

The procedure used for analysis of NO_2 absorbed in the water drop following the appropriate exposure period was the Saltzman method, adapted from ASTM 1607 (38) with N-(1-naphthyl) ethylene diamine dihychochloride as the diazotization agent. The method is actually used for determination of NO_2 in the atmosphere, but was adopted in this study due to its extreme sensitivity, i.e., 0.005 ppm to 5.0 ppm. The outstanding feature of this method is that it measures NO_2^- ion concentration directly as the calibration procedure makes use of $NaNO_2$ in aqueous solution. A detailed description of the procedure and reagents used in this procedure is given in Appendix D. This method was used rather than the standard ASTM 1607 method, the Griess - Saltzman method, because the primary reagent, α- naphthylamine, can no longer be obtained as it is carcinogenic.

Although nitrate ion is not expected to be present in significant quantity, several attempts were made to determine the amount of nitrate ion present. The most sensitive method available at present employs 1-aminopyrene (39) as the dye forming reagent. However, the presence of NO_3^- ion was not detected with the method thus indicating that either the NO_3^- ion concentration was too low to be detected, or that no significant amount of NO_3^- ion was formed.

Both methods described above are calorimetric in nature. Therefore, the Bauch and Lomb Model 10 Spectrophotometer was used for determination of absorbance at the appropriate wavelength given for each procedure.

CHAPTER IV

PROCEDURE

This chapter in conjunction with the previous chapter should give an adequate picture of the steps required to obtain data for a specific test.

First, assembling of auxiliary equipment was necessary. This involved obtaining ice and distilled, deionized water. Next, the equipment, such as the ultraviolet analyzer, the spectrophotometer, the hygrometer, and the temperature sensor and recorder were activated and allowed to warm up. Also, the temperature bath heating coil was activated and time was allowed for equilibration. Approximately thirty minutes were required for this phase.

Next, the humidity of the stream was set, depending on the supersaturation ratio which was to be observed. Supersaturation ratio (SSR) is defined by the partial pressure of the water in the tested gas divided by the partial pressure of water (4.8 mm Hg) at $5^{o}C$, the initial temperature of the droplet. The SSR's observed were 1.0, 1.5, 2.0, and 2.5 which correspond to dew point values of $5.5^{o}C$, $11.5^{o}C$, $15.5^{o}C$, and $19.5^{o}C$. To obtain these readings the values leading to and bypassing the humidifier were adjusted along with the temperature of the water bath, so that a constant $25^{o}C$ stream of desired humidity could be obtained. The dew point hygrometer was used and no NO_2 was permitted to flow while the hygrometer was in use. Therefore, N_2 was used in place of NO_2 in setting

the humidity of the flowing stream.

Next, the NO_2 line was opened and the make-up N_2 line was closed. A rotameter had been calibrated so that the amount of NO_2 to obtain 100 ppm and 300 ppm concentrations could be obtained.

The syringe was then filled with fresh cold water and allowed to equilibrate in the ice bath. The drop was then set between the two needles such that the drop was the proper size and was in contact with the thermistor such that the initial droplet temperature could be monitored.

Almost simultaneously, the solenoid valve was activated so that the humidified NO_2-air mixture would be in contact with the droplet at the $5^{o}C$ initial temperature.

The appropriate exposure time was allowed for the particular data point, either 5, 10, 15, 20, 25, 30, or 60 seconds. Due to the cumbersome nature of the apparatus, it was not possible to obtain data for shorter exposure times, although that is definitely a very interesting region of the experiment.

After the end of the exposure period a brief N_2 flushing period was allowed to remove NO_2 near the drop. Since this period, especially at low exposure times is critical, a major source of error exists here. There is no instantaneous sampling method, and therefore the extra time while the drop is sitting on the needle before it is fixed by the absorbing agent constitutes the error. Since this error can be quite significant, it is difficult to ascertain whether the quantities shown as the results in the next chapter give good quantitative results as to the actual amount of NO_2^- ion absorbed. However, the trends which are shown should be valid, as the period required for collecting the drop was kept relatively

constant.

Finally, the needle is tapped so that the exposed drop is collected into 10 ml of the absorbing agent, which immediately fixes the NO_2^- ion concentration. A fifteen to thirty minute delay is required for color development and subsequent colorimetric determination of absorbance.

The specific method for preparing the necessary reagents is given in Appendix D.

CHAPTER V

RESULTS

The experimental work was divided into two parts. The first part consisted of taking data so that a temperature-time profile of the drop as it warmed from $5^{o}C$ to its evaporation temperature could be made and compared to the temperature profile predicted theoretically by using the appropriate mass and heat transfer characteristic of the drop. The second part of the experiment consisted of using NO_2 flowing in 300 ppm and 100 ppm concentrations and testing for the concentration of NO_2^- ion in the water during the appropriate exposure times and supersaturation ratios.

The results of the first part of the experiment are indicated by Figures 3, 4, 5 and 6. The correlation for SSR's 2.5 and 2.0 were very good and needed no correction factor, while 1.5 and 1.0 SSR's required correction factors, denoted by AF in the program, of 0.235 and 0.215, respectively. The problem appeared to result from the temperature reading indicating a higher value than was theoretically possible. A detailed discussion will follow in Chapter VI.

In general, the results indicate that the computer model was satisfactory for the case when no NO_2 was flowing in the humid air stream. During these preliminary experiments, the temperature of the ambient stream, T_∞, varied from one test to the next. In later experiments, with NO_2, the ambient temperature was kept the same for all tests at $T_\infty = 25^{o}C$, as skill was gained in performing the experiment.

Table 1. Results Taken to Varify the Computer Program Tabulated Results Results Shown for Figures 3, 4, 5 and 6 Taken from Computer Program in Appendix B and Laboratory Results

SSR	Time, Sec.	Temp. °C Actually Measured	Temp. °C Predicted by Program	Wt. Drop Moles x 10^4	Reduced Temp.
2.5	5	12.0	11.1	4.571	0.38
	10	15.3	15.0	4.592	0.61
	15	17.1	17.3	4.603	0.74
	20	18.1	18.5	4.607	0.81
	30	18.9	19.4	4.606	0.86
	60	19.3	19.7	4.585	0.88
2.0	5	9.6	8.6	4.561	0.34
	10	12.9	11.9	4.576	0.58
	15	14.7	13.9	4.586	0.68
	20	16.0	15.1	4.587	0.75
	30	17.1	16.1	4.585	0.82
	60	17.6	16.5	4.561	0.85
1.5	5	11.4	11.4	4.542	0.39
	10	14.0	14.0	4.536	0.55
	15	15.6	15.5	4.523	0.65
	20	16.4	16.4	4.507	0.70
	30	16.9	17.0	4.468	0.73
	60	17.1		4.346	0.44
1.0	5	11.6	11.6	4.527	0.43
	10	13.9	13.8	4.508	0.57
	15	15.1	15.2	4.482	0.65
	20	15.6	15.7	4.454	0.68
	30	16.1	16.1	4.394	0.72
	60	16.3		4.210	0.73

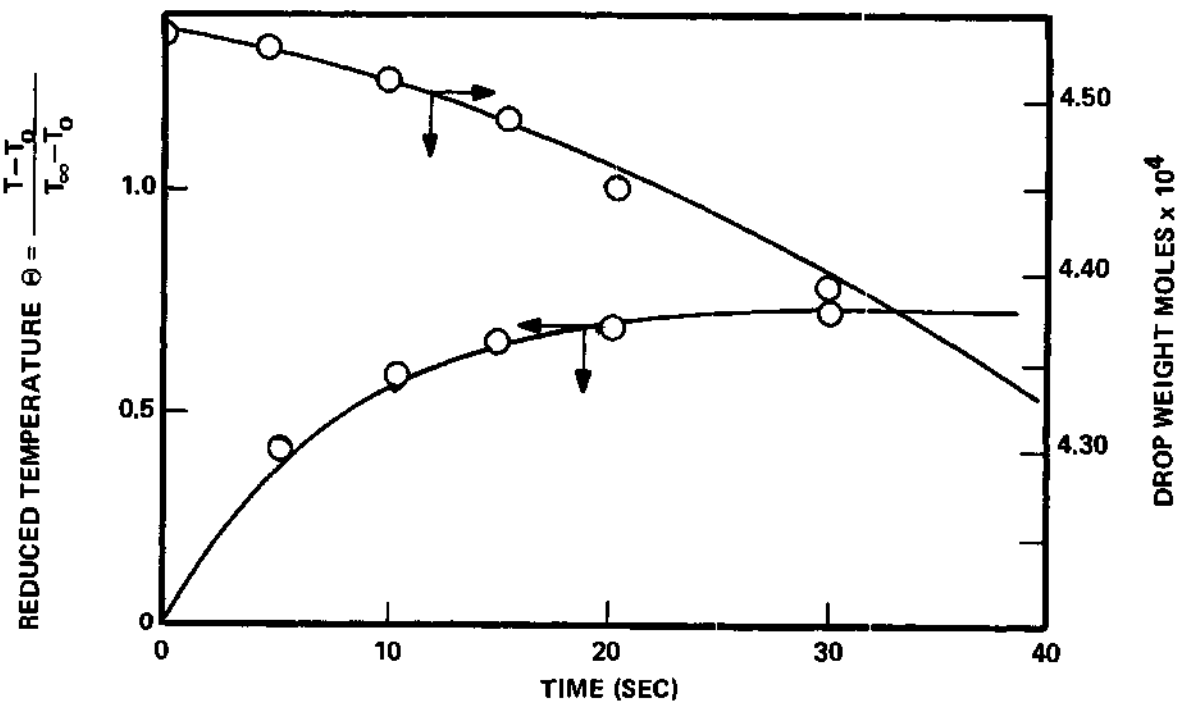

Figure 3. Reduced Temperature and Drop Weight vs. Time for SSR 1.0, T_∞ = 20.5°C

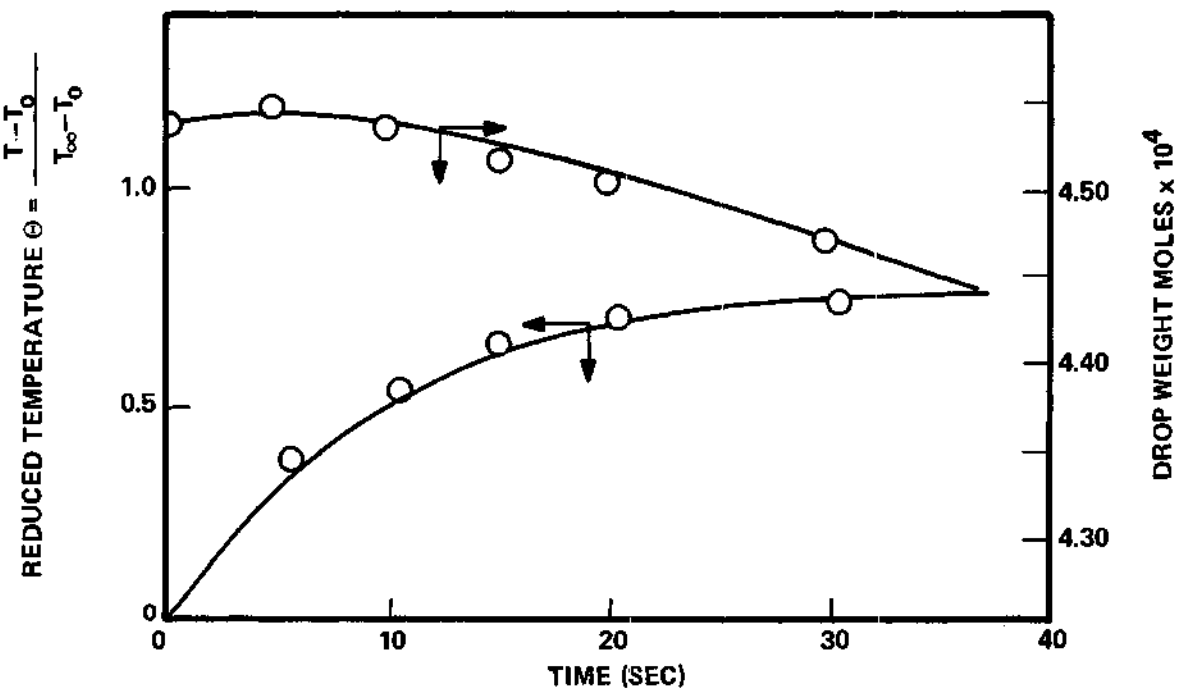

Figure 4. Reduced Temperature and Drop Weight vs. Time for SSR 1.5, T_∞ = 21.3°C

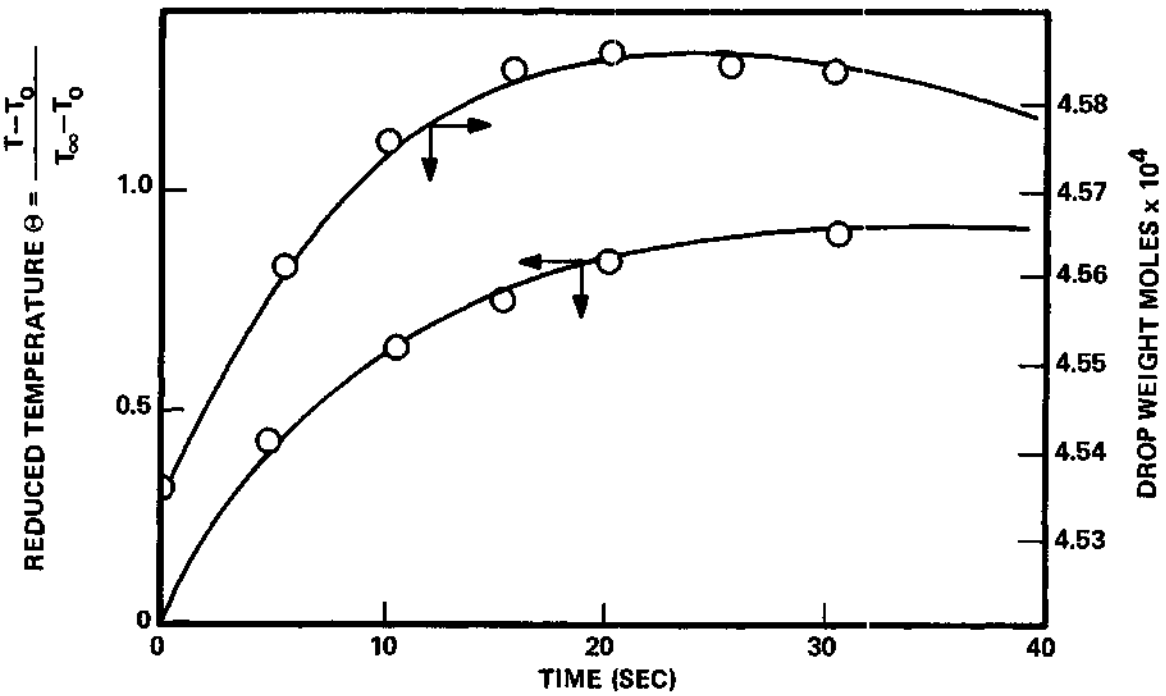

Figure 5. Reduced Temperature and Drop Weight vs. Time for SSR 2.0 T_∞ = 18.9°C

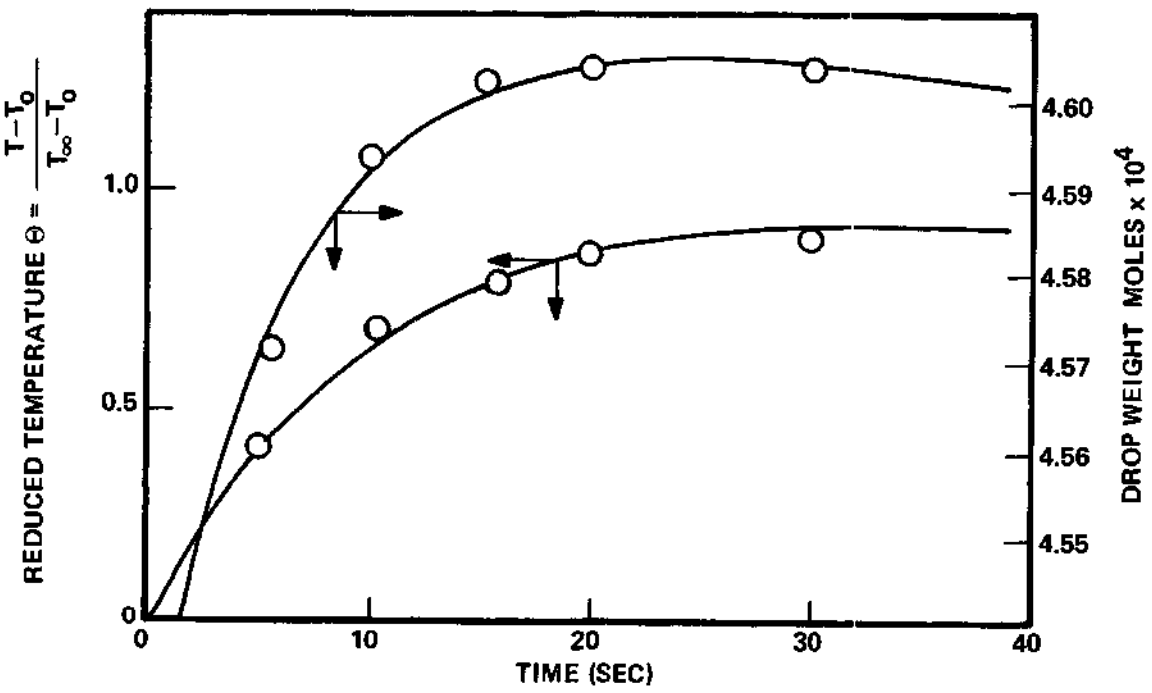

Figure 6. Reduced Temperature and Drop Weight vs. Time for SSR 2.5, $T_\infty = 21.7^oC$

With confidence in the computer program model of the temperature profile, and, therefore, with the amount of water condensed during a time interval, the second part of the experiment was undertaken. In this part, two concentrations, i.e., 300 ppm and 100 ppm, at supersaturation values of 2.5, 2.0, 1.5, and 1.0 were used and the amount of NO_2^- ion was detected. Since the ambient temperature, T_∞, was kept constant at 25^oC, Figures 7, 8, 9 and 10 indicate the temperature profiles and the amounts of H_2O condensed by use of the computer model. It should be noted that the computer model does not take into account the heat of solution, but with the low concentrations involved this effect was insignificant compared to the heating effect due to conduction and convection.

The experimental results found in the laboratory, presented as "raw data" in Appendix E, consist of a table with exposure time and absorbance data. Each data set consisted of at least three points to insure consistency of results. Data were taken until three points agreed to within 5% of one another. However, this is somewhat misleading since for data taken during the 100 ppm trials were at the very low end of the absorbance scale on the spectrophotometer. This problem will also be addressed in Chapter VI.

The tabulated and graphical results appear in Tables 1 and 2 and Figures 11 and 12, respectively. Tables 1 and 2 were derived from the raw data by using the calibration curves appearing in Appendix D. The results indicated that at the higher concentration of 300 ppm, approximately twice as much NO_2^- ion is absorbed by the drop than at 100 ppm. Also, the results indicate that increased absorbance is experienced by increased supersaturation ratio.

Table 2. Results for $T_\infty = 25^\circ C$, From Computer Program for Figures 5, 6, 7, and 8

SSR	Time	Temp.	Wt. Drop Moles x 10^4	Reduced Temp.
2.5	0	5.00	4.535	0.
	5	11.80	4.570	.34
	10	15.91	4.588	.55
	15	18.19	4.596	.66
	20	19.39	4.596	.72
	25	20.04	4.591	.75
	30	20.31	4.586	.77
	40	20.54	4.571	.78
	60	20.60	4.539	.78
2.0	5	10.61	4.557	.28
	10	14.07	4.567	.45
	15	16.06	4.567	.55
	20	17.16	4.562	.61
	25	17.79	4.553	.64
	30	18.06	4.544	.66
	40	18.31	4.521	.67
	60	18.39	4.473	.67

Table 2. Results for $T_\infty = 25^oC$, From Computer Program for Figures 5, 6, 7, and 8 Continued

SSR	Time	Temp.	Wt. Drop Moles x 10^4	Reduced Temp.
1.5	5	12.46	4.544	.37
	10	15.06	4.522	.50
	15	15.70	4.485	.54
	20	15.95	4.442	.55
	25	15.99	4.394	.55
	30	15.99	4.338	.55
1.0	0	5.0	4.535	0.
	5	11.60	4.507	.33
	10	13.07	4.445	.40
	15	13.32	4.373	.41
	20	13.36	4.287	.42
	25	13.37	4.213	.42
	30	13.37	4.126	.42

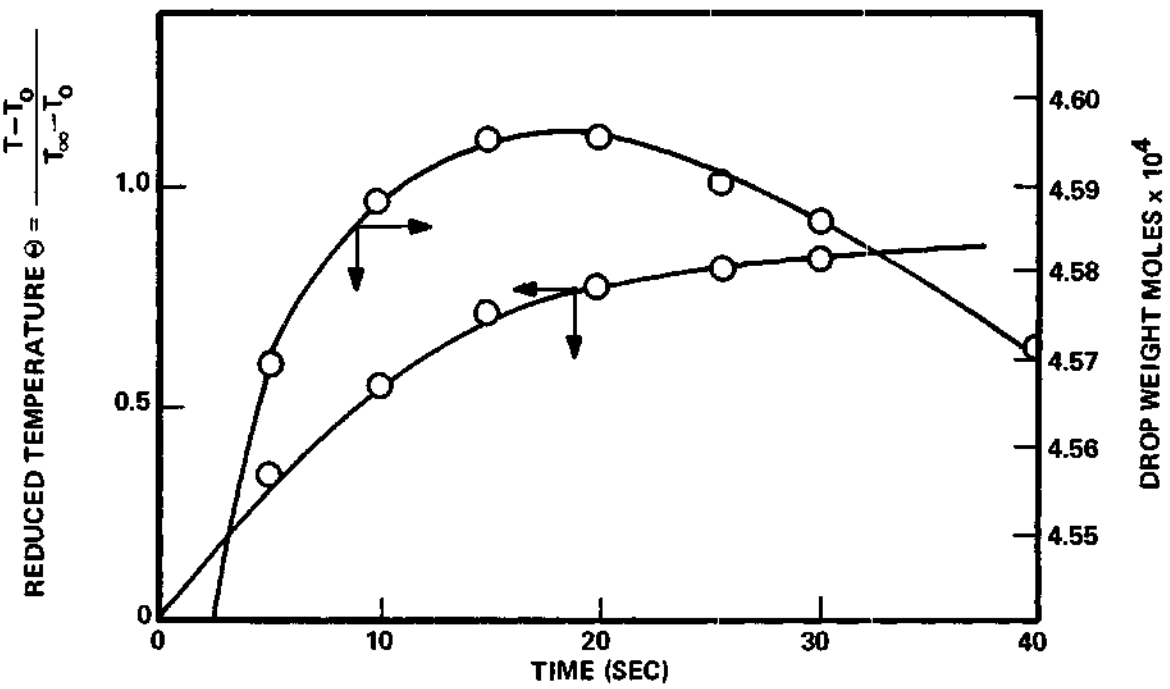

Figure 7. Reduced Temperature and Drop Weight vs. Time for SSR 2.5, $T_\infty = 25^oC$

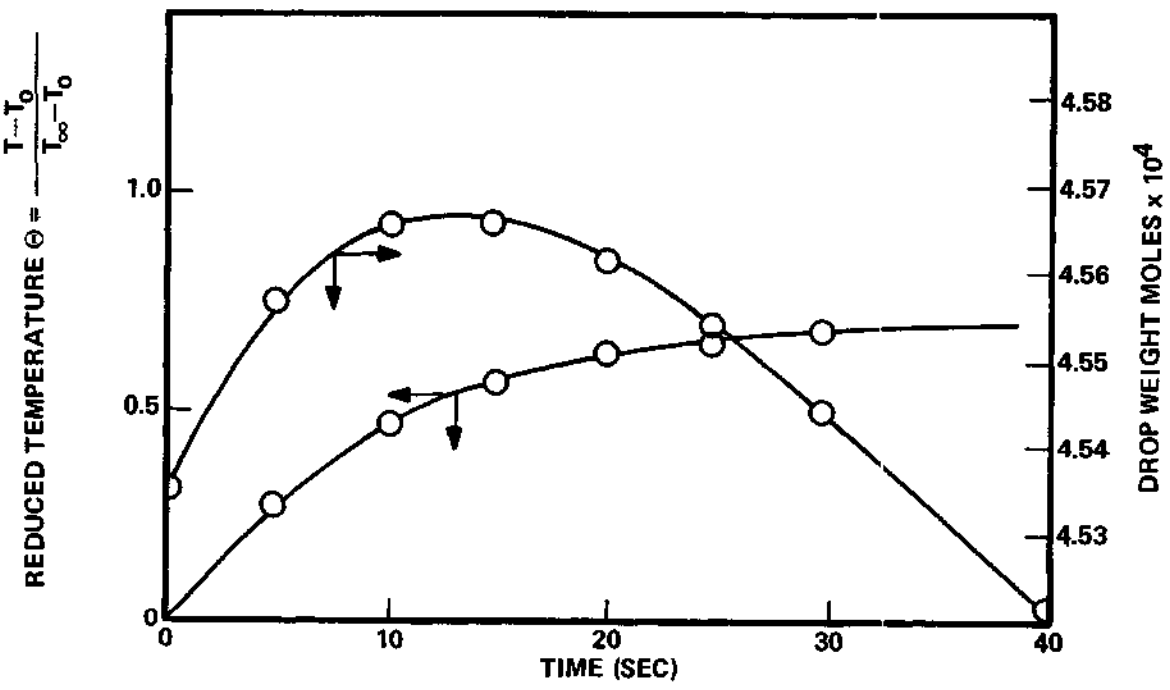

Figure 8. Reduced Temperature and Drop Weight vs. Time for SSR 2.0, $T_\infty = 25^oC$

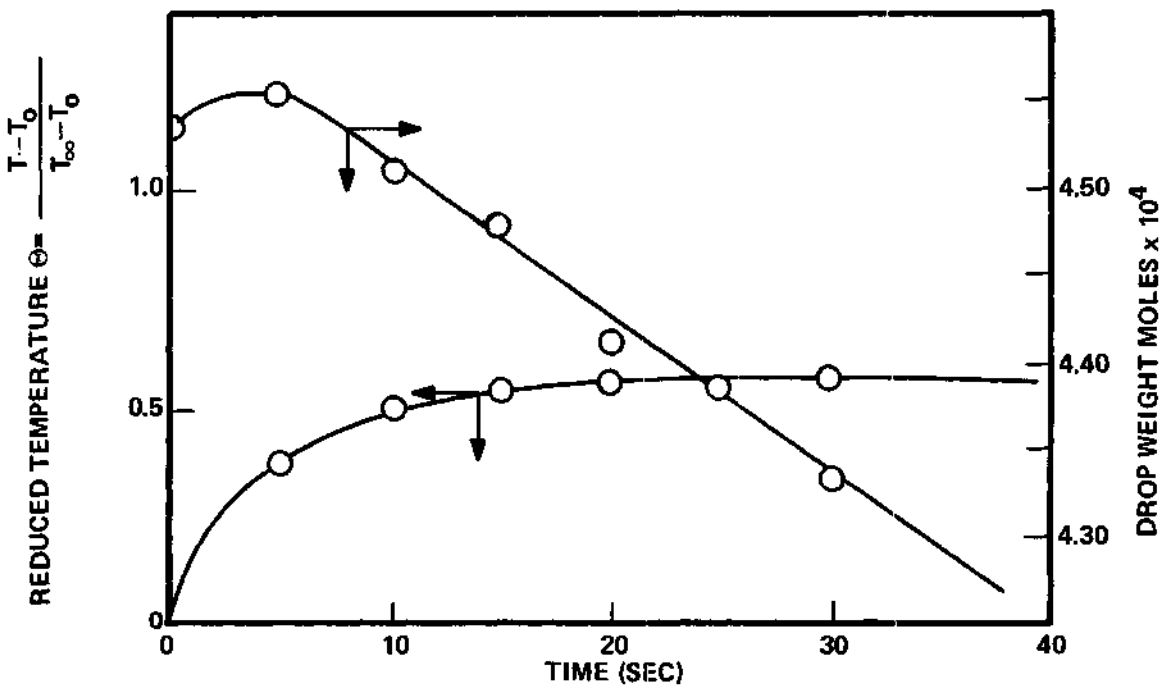

Figure 9. Reduced Temperature and Drop Weight vs. Time for SSR 1.5, $T_\infty = 25^oC$

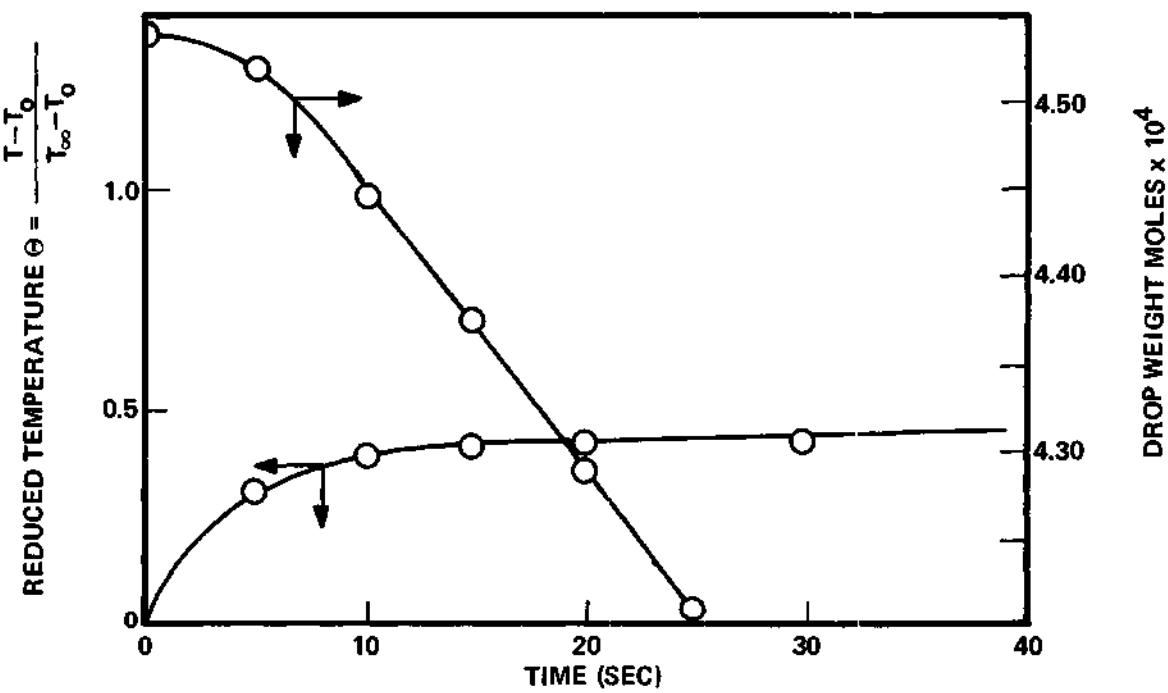

Figure 10. Reduced Temperature and Drop Weight vs. Time for SSR 1.0, T_∞ = 25°C

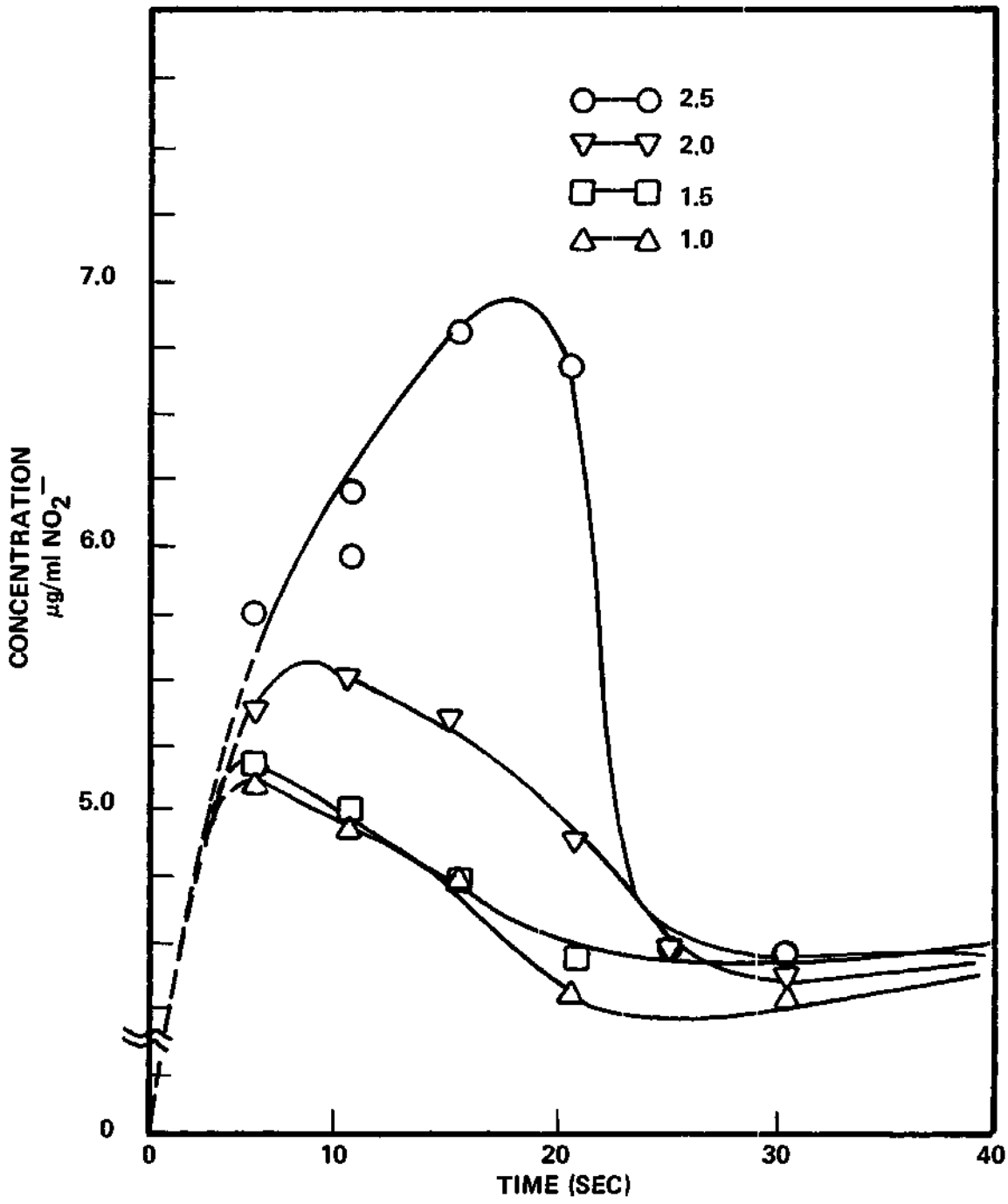

Figure 11. Experimental Results Shown on Concentration of NO_2^- ion Plotted Against Time for 300 ppm Test

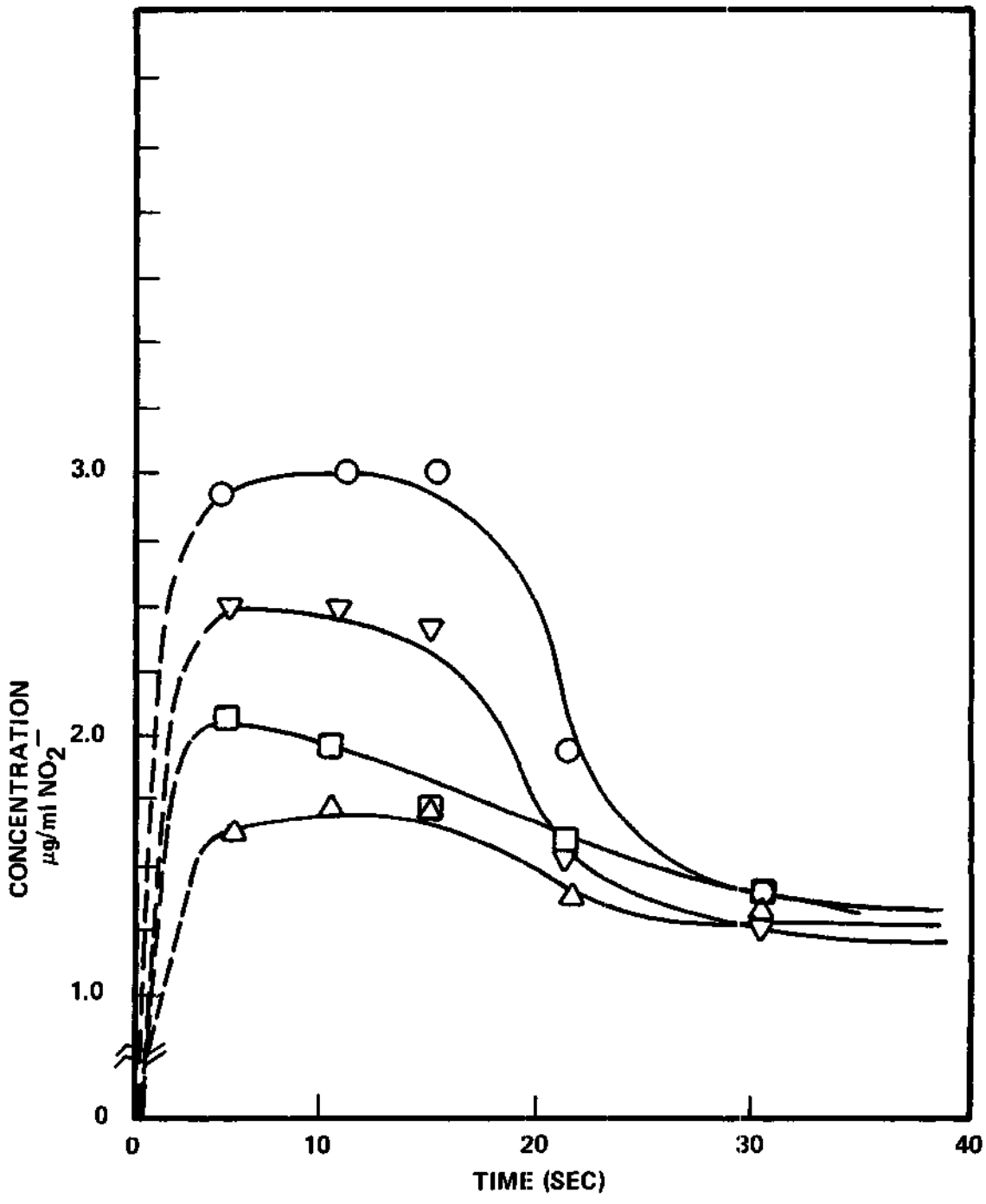

Figure 12. Experimental Results Shown on Concentration of NO_2^- ion Plotted Against Time for 100 ppm Test

According to the results, condensation occurs over the time intervals of 18, 13, 5, and 0 seconds for supersaturation ratios of 2.5, 2.0, 1.5 and 1.0, respectively. During these periods, the rates of NO_2 absorbed is greatly increased. For the first 18 seconds with SSR of 2.5 the amount of NO_2^- is shown to increase rapidly for the 300 ppm case and less rapidly 100 ppm case. However, in both cases, after 18 seconds the NO_2^- ion entrapped is apparently desorbed. The same is true for the SSR=2.0 case for the first 13 seconds and the desorption phenomena is likewise experienced. About a 10% increase in absorption is experienced by using a 2.5 SSR rather than a 2.0 SSR during the interval in which condensation is occuring for both trials. However, after 13 seconds, the 2.5 SSR absorption ratio continues to rise while desorption occurs at the 2.0 SSR. At 30 seconds, the SSR value does not appear important, as all SSR trials indicate a final value of approximately 4.2 μg NO_2^-/ml for the 300 ppm case and 1.5 μg NO_2^-/ml for the 100 ppm case. These values correspond with Borok's equilibrium values calculated by Henry's law constant of 4.51 μg NO_2^-/ml and 1.51 μg NO_2^-/ml, respectively. The results, therefore, indicate that an enhancement of nearly 52.3% over the saturation value occurred for the 300 ppm case and of 102% for the 100 ppm case at SSR = 2.5. Furthermore, at thirty seconds in all cases the final values appear to lie very closely to the saturation value predicted by Henry's law constant. Data were not taken at longer exposure time than one minute due to systematic errors discussed in Chapter VI.

Finally, it was desirable to indicate a correlation between the amount of water condensed against the amount of NO_2 absorbed within the water droplet. Due to the limited amount of time for condensation for

SSR = 2.0 and SSR = 2.5, only two reliable points, namely the 5 second and 10 second point could be used. In effect, a correlation was desired which would show the effect of condensation only rather than include other absorption methods. The preliminary results indicated that the absorption - condensation correlation was linear with slopes of 200 moles NO_2/mole H_2O and 35 moles NO_2/mole H_2O for the 300 ppm and 100 ppm cases, respectively. Obviously more data is needed before any conclusion can be reached concerning this correlation.

Figure 14 and 15, however, show that a linear relationship exists if the total amount of moles of NO_2^- absorbed is plotted against the total moles of H_2O condensed during the condensation period for the 2.5, 2.0, and 1.5 SSR cases. The slopes of these lines were 70 and 35, moles/mole respectively. It is not immediately apparent what the significance of these values is, however, it is noteworthy that the results indicate a linear relationship of absorption versus condensation over the range studied.

There is the indication that if other SSR's were studied, i.e., 1.7, or perhaps 3.0, the amount of absorption could be predicted to some extent.

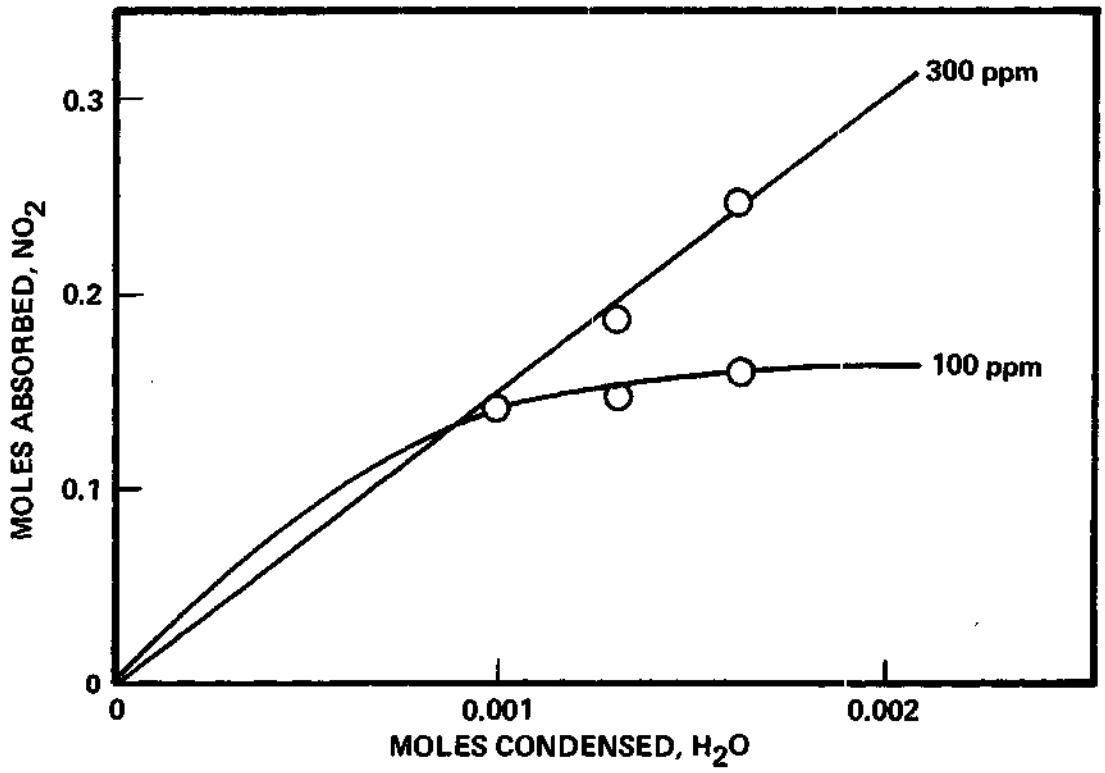

Figure 13. Moles of NO_2 Absorbed Plotted Against Moles of Water Condensed Showing Condensation Effect Only

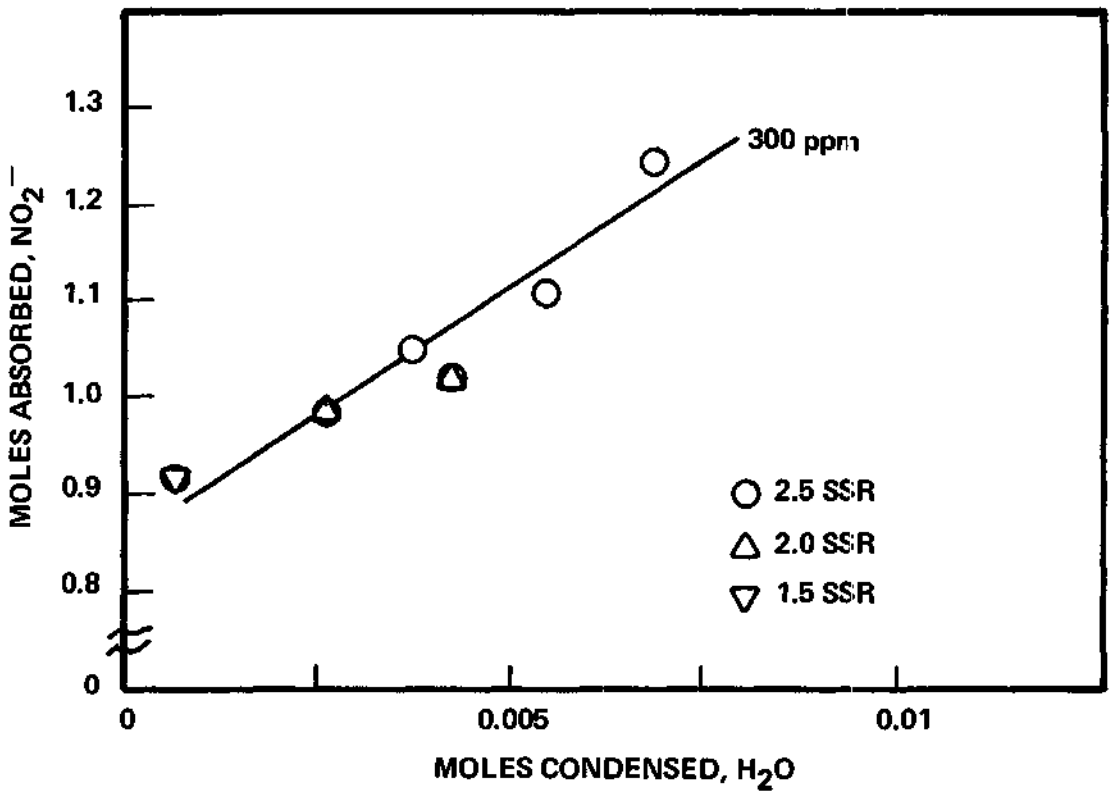

Figure 14. Moles of NO_2^- ion Absorbed Plotted Against Moles of Water Condensed Showing Condensation and Other Absorption Effects for 300 ppm Test

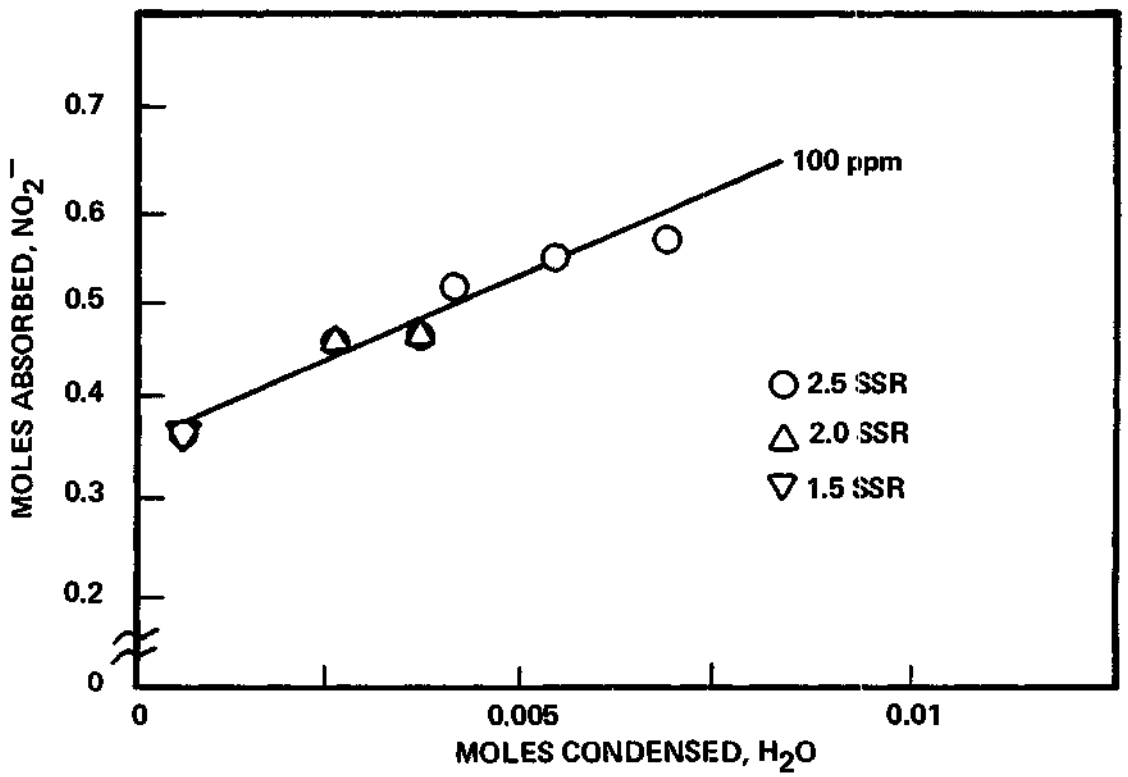

Figure 15. Moles of NO_2^- ion Absorbed Plotted Against Moles of Water Condensed Showing Condensation and Other Absorption Effects for 100 ppm Test

CHAPTER VI

DISCUSSION OF RESULTS

In the presentation of results, great emphasis was placed on the accurate representation of the data by the computer program in Appendix B. Therefore, in a discussion of systematic errors in the experiment, this would be the logical place to start.

As mentioned previously, the drop at the initial temperature of $5^{o}C$ was suspended between two 26 guage needles, one of which contained a thermistor which recorded the temperature profile. The water which was contained in the hypodermic needle was contained in an ice bath, but due to conduction of heat through the metal portion of the needle, the drop raised in temperature to $5^{o}C$. The heating of the thermistor needle is inevitable and this, therefore, introduced an error in the reading of the initial drop temperature since as the cold drop hits the termistor it is instantaneously heated by the warm thermistor needle. During the experimental measurements using the NO_2- humid air mixture of $T_\infty = 25^{o}C$, the initial temperature was recorded at $7^{o}C$. However, this was extrapolated to $5^{o}C$ in the presentation of results to account for the excess heating by the needle. Figures 2 through 10, show that T_∞ is not as significant a parameter in the temperature profile as in the water droplet mass profile. As previously mentioned, the heat of solution was not taken into account in the temperature profile and thereby in the droplet mass profile, as its contribution was deemed to be insignificant. Although

true for the species considered, it can be envisioned that for other species in which the heat of solution is significant, the results might be quite different.

The computer program indicated that the initial drop diameter was a significant parameter. In the operation of the experiment, care was taken to insure that the initial drop diameters were consistent at 0.25 cm. The spacing between the needles was such that the drop could be suspended between them at this "diameter." Further, a series of 100 drops at this diameter were collected in an ice bath to prevent evaporation and weighed and the results indicated that the average value was 0.25 cm. However, it is quite probable that on any given trial, the initial droplet diameter varied from this average value. Therefore, summarizing, the errors included in assuming the accuracy of the computer program consist of hanging a consistently sized and cooled droplet between the needles.

In the actual collection of the drop after being exposed to the NO_2- humid air stream, several considerable systematic errors exist. The first error which occured considerably at the high supersaturation ratios was fogging of the tube. Although insulated with asbestos, droplets did condense on the walls of the tube, and therefore the concentration of the gas which eventually hit the control drop may have been different from the 300 ppm and 100 ppm desired. Further, it was desirable to have a fresh cold drop be exposed simultaneously to the heated NO_2- humid air stream. Due to the nature of the apparatus, it was physically impossible to insure that this occured, and therefore, the results may have some quantitative error. To insure the coldest drop possible, the hypodermic needle was continuously purged of water and then as a drop of the desired diameter

formed, the solenoid valve was activated allowing the gas stream, already mixed, to enter the tube. Therefore, a time lag was experienced at the start of the exposure period. After the exposure period, the solenoid valve was deactivated and the NO_2- humid air flow was diverted and a short N_2 purge followed. This was done primarily for safety reasons due to the danger of NO_2 at the concentration being considered. Further, it was necessary to insure that no NO_2 was being absorbed after the designated exposure period. Following the brief N_2 purge (2 to 3 seconds), the rubber stopper below the needle was removed and depending on the condition of the tube with regard to condensate build-up, the inlet tube was dried, and the drop was then released into the collection flask. This entire procedure involved about ten seconds from the time of the exposure to the NO_2- humid air stream was ceased. Obviously, during this lag significant desorption most probably had occured, especially in the cases of short exposure time. Therefore, the results presented in Figures 11 and 12 should be viewed qualitatively rather than quantitatively to some extent. They clearly show the trend of absorption during the condensation period. The time lag for collection of the drop was consistent for each trial, but it is impossible to assess accurately the degree of the error associated with the time lag on the actual values of the absorbance values would be.

The redeeming characteristic of this error is that it should indicate low absorption values rather than high absorption values, since it is anticipated that desorption rather than absorption had occurred during the testing time interval. It has been estimated that a 10 percent error could be associated with the time lag under the most adverse conditions.

For a given data point, typically five drops were collected for

the 300 ppm concentration and ten drops were collected for the 100 ppm concentration. This was done firstly to act as an averaging method and secondly to be able to read the absorbance in the spectrophotometer at a region of the scale in which the calibration curve had been drawn, and could be read accurately. As has been clearly stated, however, individual droplets were difficult to collect and the entire collection procedure was cumbersome. Even at 10 drops, the 100 ppm data were just within the region of acceptable absorbance. Therefore, from an operational viewpoint the 100 ppm data were difficult to obtain, and somewhat unreliable.

There were no significant problems in setting other parameters, such as T_∞ and the SSR value, although at high values fogging and condensation on tubes was significant; other system constants, such as the gas velocity, merely required time and perseverance.

Other errors which must be addressed include such items as the ability to read the spectrophotometer to $\pm$ .005 units, the hygrometer to $\pm$ 0.5°F, the thermister to $\pm$ 0.5°F, and the weight of the various reagents to $\pm$ 0.0005 gm. Combined, it is very difficult to assess a value for the possible error within a specific trial. However, here the redeeming value is that the data reported here were consistant, as forced by the consistency requirement of 5% for individual data points. In other words, data were taken until at least three points were found to be within 5%. Therefore, it is contended that although the various systematic and random errors involved may cause disillusionment as to the actual values of the numbers presented, the trends which are shown here are justifiable.

Data for exposure time periods of greater than thirty seconds were difficult to obtain because the drop noticeably evaporated after twenty

seconds for all 55 cases. Particularly in the SSR = 1.0 case, after 30 seconds the drop was so small that it was difficult to tap it off the needles. Further, due to evaporation the drop had the tendency to withdraw from the second needle and this abrupt change in surface area of the drop introduced an error in the experiment. Therefore, obtaining data for exposure periods greater than sixty seconds was not possible.

CHAPTER VII

CONCLUSIONS

The mechanism of droplet growth by vapor condensation is important in concentrating trace gases in the droplet.

It is possible to have absorption during condensation in excess of the saturation value expected by Harry's law, and the subsequent desorption of the entrapped gas reverts to the saturation value within thirty seconds.

The concentration of the absorbed gas varies linearly with the amount of condensation occurring up to the point at which evaporation begins to occur.

The experiment seems to varify the hypothesis that the absorption rate is enhanced as activated sites are increased while the drop is growing and also that Stefan flow may occur during this period. Further evaporation of the drop seems to tear away the outer layers of the drop systematically, thus freeing the "trapped" gas, before significant absorption occurs, such that the concentration within the drop reverts to the saturation concentration expected by Henry's law.

CHAPTER VIII

RECOMMENDATIONS

1. It has been shown that the opportunity for enhancing absorption during condensation exists. Therefore, methods should be explored for fixing the NO_2 absorbed in the water droplet in order to avoid the return to the saturation concentration after thirty seconds.

2. An economic study should be performed to determine whether the increase in NO_2 absorption by the condensation can be favorably weighed against the cost required for a refrigeration system to obtain the initial cold droplet.

3. Although physically impossible with the apparatus used in this experiment, observations at higher supersaturation ratios would be beneficial in determining whether the straight line for moles NO_2 absorbed versus moles H_2O condensed can be extrapolated to higher values.

4. The NO species should be explored as it is a direct product of combustion processed, whereas NO_2 is the result of oxidation of NO after a period of time in the atmosphere. It might be possible to add an NO scrubber using the condensation principle directly to existing NO sources and avoid NO_2 formation in the atmosphere.

APPENDIX A

NOMENCLATURE

APPENDIX A

NOMENCLATURE

A	Surface area of drop [cm^2]
$C_{A\ell}$	Concentration of component A in water [gr mole/cm^3]
C_{Ao}	Initial concentration of component A [gr mole/cm^3]
C_{Ag}	Concentration of component A in fluid stream [gr mole/cm^3]
C_{pA}	Heat capacity of component A [cal/gr^oK]
D_d	Diameter of drop [cm]
D_A	Diffusivity of component A [cm^2/sec]
H	Henry's law constant
h_m	Heat transfer coefficient [cal/cm^2sec-^oK]
K_x	Mass transfer coefficient [gr/cm^2-sec]
k_A	Thermal conductivity of component A [cal/gr^oK]
m	Mass of drop [gr]
N_A	Diffusional molar flux [gr-mole/cm^2--sec]
Nu	Nusselt Number
P	Vapor pressure of water (mm Hg)
Pr	Pandtl Number
P_T	Total Pressure (mm Hg)
Sc	Schmidt Number
Sh	Sherwood Number
T	Temperature of drop (^oC)
θ	Time

T_i Initial temperature of drop (^{o}C)

T_f Final temperature of drop (^{o}C)

V_d Volume of drop (cm^3)

V Velocity of air stream (cm/sec)

W Rate of condensation (gr/sec)

X Distance from interface to bulk (cm)

ρ_A Density of component A . (gr/cm^3)

μ_A Viscosity of component A . (gr/cm-sec)

λ Heat of condensation (cal/gr)

α Thermal diffusivity (cm^2/sec)

APPENDIX B

COMPUTER PROGRAM LOGIC OUTPUT

APPENDIX B

COMPUTER PROGRAM LOGIC OUTPUT

The computer program, and the logic sequence used to obtain the program was prepared by Mark Beshears and revised by the author. It is presented in this Appendix.

The output of the program is shown in a condensed version in Table 1, and is compared to the laboratory data obtained for the temperature profile of the drop.

An energy balance over the drop yields

$$\frac{d[mC_p[T_s-T_{ref}]]}{dt} = mC_p \frac{d\,[T_s-T_{ref}]}{dt} + m[T_s-T_{ref}] \left[\frac{dP}{dt}\right]$$

$$+ C_p\,[T_s-T_{ref}]\,\frac{dm}{dt}$$

$= h_X A\,[T_\infty - T]$ Heat transfer by connection

$+ W\Delta H$ Heat transfer by condensation of liquid

$+ WM_w C_p[T_s-T_{ref}]$ Enthalpy of condensed water

If we assume that C_p is constant over the temperature range in question, then the $\frac{dC_p}{dt}$ term drops out.

Also, since W, the molar condensation rate is equivalent to $\frac{1}{M_w}\frac{dm}{dt}$ the relation reduces to

$$MC_p \frac{d[T_s-T_{ref}]}{dt} = mC_p \frac{dTs}{dt} = h_X A\,[T_\infty - T_s] + W_\infty \Delta H$$

Now for W we use the relation

$$W = \frac{dM}{dt} = k_X A\,\frac{[X_\infty - X_s]}{[1 - X_s]}$$

$$\frac{dTs}{dt} = \frac{A}{mC_p}\left[k_x \Delta H_v \left[\frac{X_\infty - X_s}{1-X_s}\right] + h_x[T_\infty - T_s]\right]$$

Now, $A = \pi D_d^2 \qquad M = V\rho$

$$V = \frac{\pi D_d^3}{6} \qquad \frac{A}{mC_p} = \frac{\pi D_d^2}{\frac{D_d^3}{6} C_p \pi \rho} = \frac{6}{D_d \rho C_p}$$

Also, $V = \frac{m}{\rho} = \frac{D_d^3}{6}$ Note: Here P&C_p are for liquid water.

$$D_d = \left[\frac{6M}{\pi\rho}\right]^{\frac{1}{3}} = \left[\frac{6M_w M}{\pi\rho}\right]^{\frac{1}{3}}$$

$$A = \pi\left[\frac{6M_w M}{\pi\rho}\right]^{\frac{2}{3}} ; \frac{A}{mC_p} = \frac{6}{C_p}\left[\frac{6M_w M}{\pi\rho}\right]^{-\frac{1}{3}}$$

$$\frac{dTs}{dt} = \frac{6}{\rho C_p}\left[\frac{6M_w M}{\pi\rho}\right]^{\frac{1}{3}}\left[K_x \Delta H_v \left[\frac{X_\infty - X_s}{1-Xs}\right] + h_X \left[T_\infty - Ts\right]\right]$$

Now set $\frac{h_x 6}{\rho C_p}\left[\frac{6M_w}{\pi\rho}\right]^{-\frac{1}{3}} = \delta$

$$\frac{[K_x \Delta H_v]}{[h_x]} = \beta$$

$$\frac{dTs}{dt} = \delta[M]^{\frac{-1}{3}} \left[\frac{\beta\,[X_\infty - Xs]}{[1-Xs\,]} + T_\infty - Ts \right]$$

Now for W

$$W = K_x \Pi \left[\frac{6M_w M}{\Pi\rho\,}\right]^{\frac{2}{3}} \left[\frac{X_\infty - Xs}{1-Xs\,}\right]$$

$$\text{Set} \quad \alpha = K_x\, \pi \left[\frac{6M_w}{\pi\rho\,}\right]^{\frac{2}{3}}$$

$$W = \frac{dM}{dt} = \alpha M^{\frac{2}{3}} \left[\frac{X_\infty - Xs}{1-Xs\,}\right]$$

We now have two coupled differential equations which can be treated with the 4th order Runga Kutta method, which is a step procedure that calculates values for T_s and M @ given intervals of t:

Using literature values we can develop relations for ΔH_v, X_x, h_x, and X_s as functions of T_s using second order power series.

Assuming the air @ the air-water interface is saturated we fit vapor pressure data from the 1967 ASME tables to the equation for

$$\ln V\,H_2O = a_o + a_1 T_s + a_2 T_s^{\,2}$$

then assuming atmospheric pressure of 740 mm Hg we have

$$X_{H_2O} = X_s = a_3\, e^{[a_o + a_1\, T_s + a_2\, T_s^{\,2}]}$$

Where

$$a_o = 6.9885 \times 10^{-2}$$

$$a_1 = 1.5216$$

$$a_2 = 0.07259$$

$$a_3 = 0.000274$$

Again using the 1967 ASME steam tables the molar heat of evaporation, ΔH_v , was fit to the equation form

$$b_o + b_1 T_s + b_2 T_s^2 \left[= \right] \frac{\text{cal}}{\text{gmol}}$$

Where

$$b_o = 10767.6$$

$$b_1 = -1.03579 \times 10^{+1}$$

$$b_2 = 7.87052 \times 10^{-3}$$

For the molar mass transfer coefficient we use

$$\frac{K_x D_d}{D_{AB}^C} = 1.13 \, Re^{\frac{1}{2}} \, Sc^{\frac{1}{3}}$$

Where $Re = \frac{D_d v \rho_g}{\mu_g}$, $Sc = \frac{\mu_g}{\rho_g D_{AB}}$.

and $$D_{AB} = \frac{\left[a \left[\frac{T_f}{T_{C_A} T_{C_B}} \right]^b \left[P_{C_A} P_{C_A} \right]^{\frac{1}{3}} \left[T_{C_A} T_{C_A} \right]^{\frac{5}{12}} \left[\frac{1}{M_A} + \frac{1}{M_B} \right]^{\frac{1}{2}} \right]}{P}$$

Where

$$a = 3.64 \times 10^{-4}$$

$$b = 2.334$$

ρ_g is calculated as

$$\rho_g = \frac{PM_w}{RT_f z} = \frac{P}{RT_f} \left[M_{W_B} z_B [1-X_s] + M_{W_A} z_A X_S \right]$$

μ_g is calculated as

$$\mu_g = \frac{\left[\mu_B [1-X_s] M_{W_B}^{\frac{1}{2}} + \mu_A X_s M_{W_A}^{\frac{1}{2}} \right]}{\left[[1-X_s] M_{W_B}^{\frac{1}{2}} + X_s M_{W_A}^{\frac{1}{2}} \right]}$$

Literature values of μ_g and μ_A were fitted to second order equations as functions of T_s where:

$$\mu = \mu_{oi} + \mu_{1i} T_f + \mu_{2i} T_f^2 \quad [=] \frac{gm}{cm\ sec}$$

for H_2O cm sec $\mu_{OA} = 8.851 \times 10^{-5}$

$\mu_{1A} = 4.813 \times 10^{-7}$

$\mu_{2A} = 2.177 \times 10^{-9}$

for air $\mu_{OB} = 1.708 \times 10^{-4}$

$\mu_{1B} = 8.011 \times 10^{-7}$

$\mu_{2B} = 7.778 \times 10^{-9}$

For the heat transfer coefficient we use the relation

$$h_x D_d = 2.0 + .60\ Re^{\frac{1}{2}}\ Pr^{\frac{1}{3}}$$

where

$$Pr = \frac{C_{P_g}\ \rho_g}{K_g}$$

C_{P_g} is calculated as

$$C_{P_g} = [1-Xs]\ C_{P_b} + X_s\ C_{P_A}\ [=]\ \frac{cal}{gm^oC}$$

literature values for the coefficients of power equations for the molar heat capacities of air and H_2O vapor were used.

$$C_{P_A} = \frac{\left[\ 7.880 + 3.2 \times 10^{-3} T_4 - 4.83 \times 10^{-7}\ T_f^{\,2}\ \right]}{18.02}\ [=]\ \frac{cal}{gm^oC}$$

$$C_{P_B} = \frac{\left[\ 6.917 + 9.911 \times 10^{-4} T_F + 7.627 \times 10^{-7} T_f^{\,2} - 4.696 \times 10^{-10} T_f^{\,3}\ \right]}{28.97}$$

K_g is calculated as

$$K_g = \frac{[1-Xs]\ K_B\ M_{W_B}^{\frac{1}{3}} + X_s\ K_A\ M_{W_A}^{\frac{1}{3}}}{[1-Xs]\ M_{W_B}^{\frac{1}{3}} + X_s\ M_{W_A}^{\frac{1}{3}}}\ [=]\ \frac{cal}{cm\ sec^oC}$$

Literature values K_A & K_B were fitted to record order equations as functions of T_S where:

$$K_i = C_{oi} + C_{1i}\, T_f + C_{2i}\, T_f^2 \quad [=] \quad \frac{cal}{cm\ sec\ ^oC}$$

for H_2O vapor $\quad C_{OA} = 3.790 \times 10^{-5}$

$$C_{1A} = 1.913 \times 10^{-7}$$

$$C_{2A} = 0.0$$

for air $\quad C_{OB} = 5.750 \times 10^{-5}$

$$C_{1B} = 1.867 \times 10^{-7}$$

$$C_{2B} = -3.856 \times 10^{-9}$$

Note: ρ_g, μ_g, C_{P_g}, K_g are calculated @ a temperature

$$T_f = \frac{[T_\infty + Ts]}{[\ 2\ ]} \quad [=] \ ^oC$$

Values used in the calculations:

$$\rho = 740 \text{ mm Hg}$$

$$C_{P_{H_2O}} = 1.000 \ \frac{cal}{gm\ ^oC}$$

$$\rho_{H_2O} = .9999 \ \frac{gm}{cm^3}$$

$$M_{W_B} = 28.97 \ \frac{gm}{gmole}$$

$M_{W_A} = 18.02 \ \frac{gm}{gmol}$

$T_{C_A} = 674.4^{o}K$

$T_{C_B} = 132.5 \ ^{o}K$

$P_{C_A} = 218.4$ atm

$P_{C_B} = 37.2$ atm

$V = 50 \ \frac{cm}{sec}$

$D_P = .25$ cm

This procedure modeled the 2.5 and 2.0 S.S.R. data satisfactorily yet failed in the 1.5 and 1.0 S.S.R. cases.

To model the 1.5 and 1.0 S.S.R. cases the heat transfer coefficient, h_x, is multiplied by a factor TF_h. TF_h, a function of t, grows exponentially from time equal zero to time equal thirty-one seconds. At which time the value of TF_h is frozen and kept constant.

For S.S.R. = 1.0 $TF_h = 2.7597 \ e^{.01361t} + .215 \quad t < 31$ sec

TF_h = Constant $\quad t > 31$ sec

For S.S.R. = 1.5 $TF_h = 1.8097 \ e^{.01707e} + .235 \quad t < 31$ sec

TF_h = Constant $\quad t > 31$ sec

This multiplication factor was developed by finding the value of TF_h @ a certain time that would fit the model value to a smoothed data value taken from a curve drawn to the data. This was done for times of 3, 6, 9, 12, 15, 18, 24, and 30 secs. It was found that the values of $\ln TF_h$ for 9 through 30 secs were linear as functions of time. The lack of linearity for times less than 9 seconds is compensated for by the addition constant; .215 for the S.S.R. = 1.0 case and .235 for the S.S.R. = 1.5 case

Subscripts:

A = H_2O vapor

B = air

C = total gas phase

```
PROGRAM-WMBSP    73/74  OPT=1                    FTN 4.6+428    77/05/23. 15.41.34    PAGE    1

      1          PROGRAM WMBSP(INPUT,OUTPUT,TAPE5=INPUT,TAPE6=OUTPUT)
                C
                C     THIS PROGRAM CALCULATES FOR A WATER DROP SUSPENDED IN A HUMID
                C     AIR STREAM THE :  DROP TEMP. , SEC = TS
      5         C                       MOLES WATER IN DROP , GMOLES = M
                C                  AND  CONDENSATION RATE , GMOLES/SEC = W
                C     AS FUNCTIONS TIME
                C
                REAL M ,MKM(5),MKTS(5),MIRANS
     10         *READ(5,5000) A0,A1,A2,A3,B0,B1,B2,UA0,UA1,UA2,UM0,UM1,UM2,CPA0,
                *CPA1,CPA2,CPA3,CPW0,CPW1,CPW2,AK0,AK1,AK2,WK0,WK1,TOTTIM,DELTIM,
                *V,TOREF ,TIMEZ
                READ(5,5000) DIAM,T0,TINF,SSR,TFA,TFB,TFC
                READ(5,5000) TOT
     15         C
                C     VARIABLE LIST      TOTTIM = TOTAL TIME SPAN , SEC
                C                        DELTIM = TIME INCREMENT , SEC
                C                        V = VELOCITY OF AIR STREAM , CM/SEC
     20         C                        TOREF = TEMP. AT WHICH SSR IS CAL. , DEG. C
                C                        TIMEZ = INITIAL TIME , SEC
                C                        DIAM = INITIAL DROP DIAMETER , CM
                C                        T0 = INITIAL DROP TEMP. , DEG. C
                C                        TINF = BULK TEMP. , DEG. C
     25         C                        SSR = SUPERSATURATION RATIO
                C                        TOT = TIME AT WHICH TF IS FROZEN , SEC
                WRITE(6,6000)
                C
     30         C     INITIALIZATION OF VALUES
                C
                W = 0.0
                M = 2.9027E-02 * (DIAM**3)
                TS = T0
                TIME = TIMEZ
     35         C
                C     CALCULATION OF AIR STREAM WATER MOLE FRACTION , XINF
                C
                XINF = SSR *(A0+EXP(A0 + A1*TOREF + A2*TOREF**2))
                N = TOTTIM / DELTIM + 1.
     40         C
                C     RUNGA KUTTA LOOP
                C
                DO77 I=1,N
                WRITE(6,6000) TIME , TS , M , W , MDELT , TF
     45         IF(I.EQ.N)  GO TO 9999
                CA1 = TS
                CA2 = M
                DO55 K=1,4
                C
     50         C     CALCULATION OF WATER-MOLE FRACTION OF AIR AT DROP SURFACE
                C
                XS = A3 * EXP( A0 + A1*CA1 + A2*CA1**2)
                G = ( XINF - XS ) / ( 1. - XS )
     55         C
                C     CALCULATION OF MOLAR HEAT OF VAPORIZATION , CAL/GMOLE
                C
                DELHV = B0 + B1*CA1 + B2*CA1**2
```

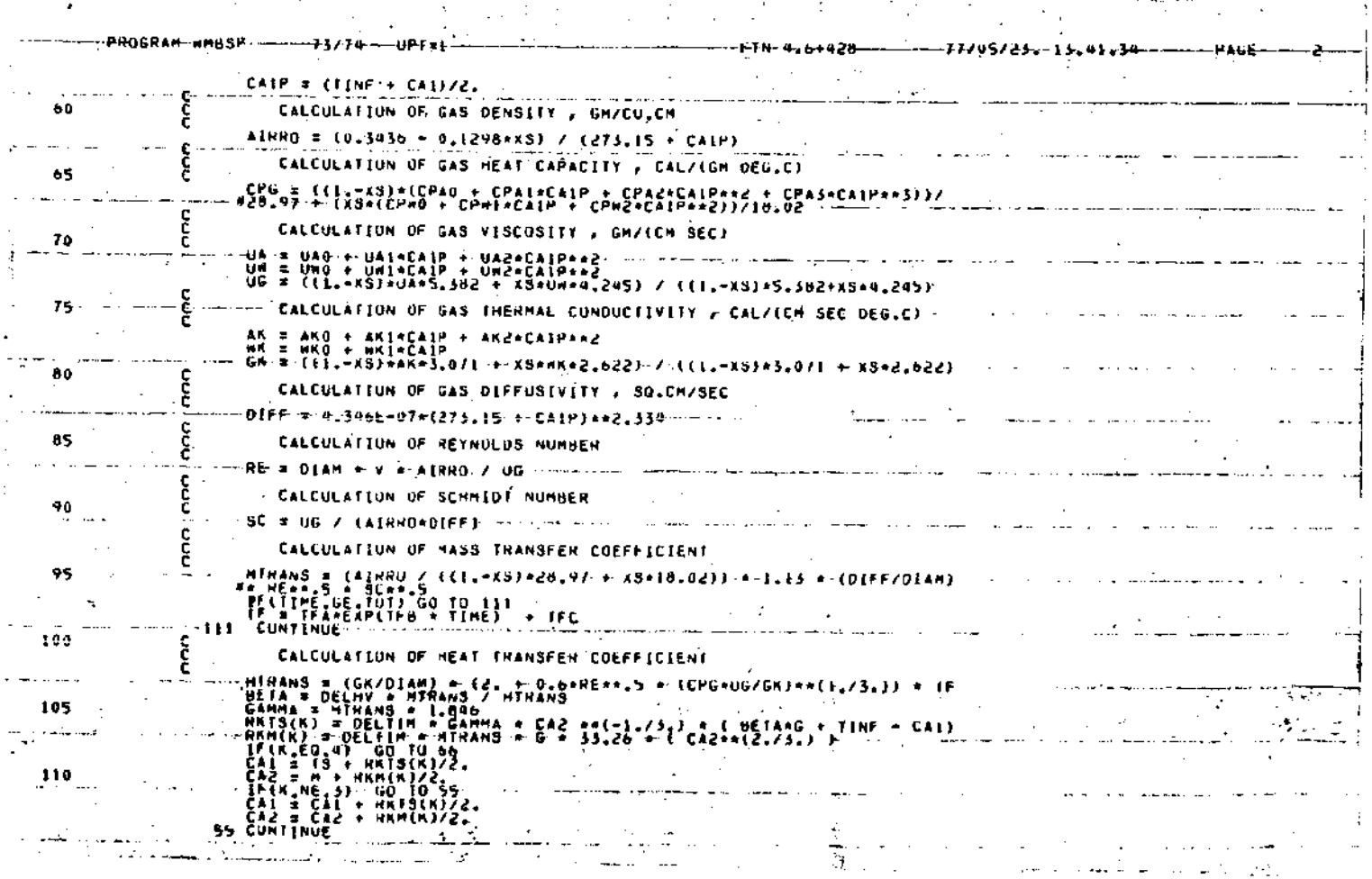

```
PROGRAM HMBSR    73/74  OPT=1                    FTN 4.6+428    77/05/25. 15.41.34    PAGE    2

      CAIP = (TINF + CAI)/2.
C
C        CALCULATION OF GAS DENSITY , GM/CU.CM
C
      AIRRO = (0.3936 + 0.1298*XS) / (273.15 + CAIP)
C
C        CALCULATION OF GAS HEAT CAPACITY , CAL/(GM DEG.C)
C
      CPG = ((1.-XS)*(CPA0 + CPA1*CAIP + CPA2*CAIP**2 + CPA3*CAIP**3))/
     #28.97 + (XS*(CPW0 + CPW1*CAIP + CPW2*CAIP**2))/18.02
C
C        CALCULATION OF GAS VISCOSITY , GM/(CM SEC)
C
      UA = UA0 + UA1*CAIP + UA2*CAIP**2
      UW = UW0 + UW1*CAIP + UW2*CAIP**2
      UG = ((1.-XS)*UA*5.382 + XS*UW*4.245) / ((1.-XS)*5.382+XS*4.245)
C
C        CALCULATION OF GAS THERMAL CONDUCTIVITY , CAL/(CM SEC DEG.C)
C
      AK = AK0 + AK1*CAIP + AK2*CAIP**2
      WK = WK0 + WK1*CAIP
      GK = ((1.-XS)*AK*3.071 + XS*WK*2.622) / ((1.-XS)*3.071 + XS*2.622)
C
C        CALCULATION OF GAS DIFFUSIVITY , SQ.CM/SEC
C
      DIFF = 4.306E-07*(273.15 + CAIP)**2.334
C
C        CALCULATION OF REYNOLDS NUMBER
C
      RE = DIAM * V * AIRRO / UG
C
C        CALCULATION OF SCHMIDT NUMBER
C
      SC = UG / (AIRRO*DIFF)
C
C        CALCULATION OF MASS TRANSFER COEFFICIENT
C
      MTRANS = (AIRRO / ((1.-XS)*28.97 + XS*18.02)) * 1.15 * (DIFF/DIAM)
     #* RE**.5 * SC**.5
      IF(TIME.GE.TUT) GO TO 111
      IF = IFA*EXP(IFB * TIME)  + IFC
  111 CONTINUE
C
C        CALCULATION OF HEAT TRANSFER COEFFICIENT
C
      HTRANS = (GK/DIAM) * (2. + 0.6*RE**.5 * (CPG*UG/GK)**(1./3.)) * IF
      BETA = DELHV * MTRANS / HTRANS
      GAMMA = HTRANS * 1.006
      HKTS(K) = DELTIM * GAMMA * CA2 **(-1./3.) * ( BETA*G + TINF - CAI)
      HKM(K) = DELTIM * MTRANS * G * 33.26 * ( CA2**(2./3.) )
      IF(K.EQ.4)  GO TO 66
      CAI = TS + HKTS(K)/2.
      CA2 = M + HKM(K)/2.
      IF(K.NE.3)  GO TO 55
      CAI = CAI + HKTS(K)/2.
      CA2 = CA2 + HKM(K)/2.
   55 CONTINUE
```

```
      PROGRAM WMBSP      73/74   OPT=1                    FTN 4.6+428      77/05/23. 13.41.34      PAGE    3

  115           66 TS = TS + (RKTS(1) + 2.*RKTS(2) + 2.*RKTS(3) + RKTS(4)) / 6.
                   WDELT = ( RKM(1) + 2.*RKM(2) + 2.*RKM(3) + RKM(4) )/6.
                   M = M + WDELT
                   W = WDELT / DELTIM
                   TIME = TIME + DELTIM
  120           77 CONTINUE
                9999 WRITE(6,6667) DIAM ,SSR,TO,TINF,DELTIM
                   PRINT*,CPG,GK,UG
                   PRINT*,SC,RE,AIRRO
                   PRINT*,MTRANS,MTRANS,DELMV
  125           5000 FORMAT(4E20.5)
                6000 FORMAT (1H1,13X,"TIME",7X,"DROP TEMP.",7X,"MOLES DROP",7X,
                   # "CONDENS. RATE",5X,"MOLES CONDENSED IN",7X,"TF",//,14X,"(SEC)",
                   # 7X,"(DEG. C)",27X,"(MOLES/SEC)",9X,"TIME INTERVAL",//)
                6666 FORMAT(1HA,12X,F5.1,9X,F5.2,4(8X,E12.6,))
  130           6667 FORMAT(1HA,//,12X,"DROP DIAMETER = ",F5.2," CM.",//,12X,"S.S.R. =
                   #",F5.1,//,12X,"INITIAL DROP TEMP. = ",F5.1,"DEG.C",//,12X,
                   #"BULK TEMP. = ",F5.1," DEG.C",///,12X,"TIME INTERVAL = ",F5.3,///)
                   END


     SYMBOLIC REFERENCE MAP (R=1)

ENTRY POINTS
1114  WMBSP

VARIABLES     SN  TYPE            RELOCATION

1733  AIRRO       REAL                          4740  AK          REAL
1672  AK0         REAL                          4675  AK1         REAL
1674  AK2         REAL                          4646  A0          REAL
1647  A1          REAL                          4650  A2          REAL
1651  A3          REAL                          4747  BETA        REAL
1652  B0          REAL                          4653  B1          REAL
1654  B2          REAL                          4724  CA1         REAL
1732  CAIP        REAL                          4725  CA2         REAL
1663  CPA0        REAL                          4664  CPA1        REAL
1665  CPA2        REAL                          4666  CPA3        REAL
1734  CPG         REAL                          4667  CPW0        REAL
1670  CPW1        REAL                          4671  CPW2        REAL
1731  DELMV       REAL                          4700  DELTIM      REAL
1704  DIAM        REAL                          4743  DIFF        REAL
1730  G           REAL                          4750  GAMMA       REAL
1742  GK          REAL                          4746  HTRANS      REAL
1721  I           INTEGER                       4726  K           INTEGER
1644  M           REAL                          4645  MTRANS      REAL
1720  N           INTEGER                       4744  NE          REAL
1751  RKM         REAL        ARRAY             4756  RKTS        REAL        ARRAY
1745  SC          REAL                          4707  SSR         REAL
1723  TF          REAL                          4710  TFA         REAL
1711  TFB         REAL                          4712  TFC         REAL
1716  TIME        REAL                          4703  TIMEZ       REAL
1706  TINF        REAL                          4702  TOREF       REAL
1713  TOT         REAL                          4677  TOTTIM      REAL
1715  TS          REAL                          4705  TO          REAL
```

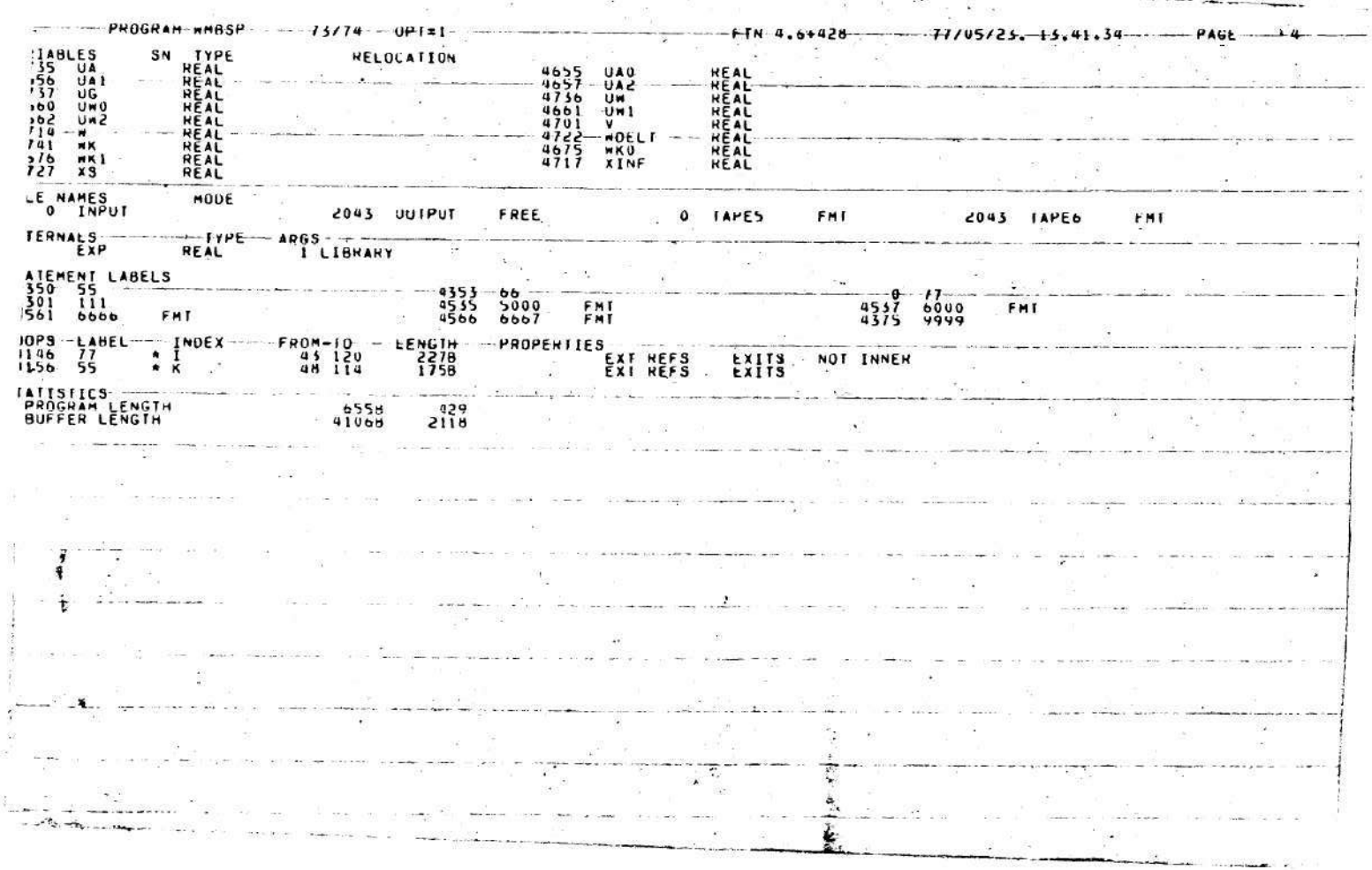

```
PROGRAM WMBSP    73/74  OPT=1                    FTN 4.6+428    77/05/25. 15.41.34    PAGE  4

IABLES      SN  TYPE          RELOCATION
 35  UA         REAL                          4655  UA0        REAL
 56  UA1        REAL                          4657  UA2        REAL
 37  UG         REAL                          4736  UM         REAL
 60  UM0        REAL                          4661  UM1        REAL
 62  UM2        REAL                          4701  V          REAL
 14  W          REAL                          4722  WDELT      REAL
 41  WK         REAL                          4675  WK0        REAL
 76  WK1        REAL                          4717  XINF       REAL
 27  XS         REAL

LE NAMES        MODE
   0  INPUT                  2043  OUTPUT    FREE          0  TAPES    FMT          2043  TAPE6    FMT

TERNALS         TYPE   ARGS
      EXP       REAL     1 LIBRARY

AIEMENT LABELS
 350  55                              4353  66                                0  77
 301  111                             4535  5000     FMT                  4537  6000     FMT
 561  6666     FMT                    4566  6667     FMT                  4375  9999

OPS  LABEL   INDEX     FROM-ID   LENGTH   PROPERTIES
1146  77     * I         45 120     2278              EXT REFS    EXITS   NOT INNER
1156  55     * K         48 114     1758              EXT REFS    EXITS

TATISTICS
 PROGRAM LENGTH              6558     429
 BUFFER LENGTH              41088    2118
```

Computer Program (continued)

APPENDIX C

DETERMINATION OF HENRY'S LAW CONSTANT

The Henry's law constant calculated from Borok's work was calculated to be 100 atm (See Figure C-1). This value indicates total NO_2 dissolved in H_2O.

In this study, NO_2^- ion was detected in water, as discussed in Appendix D. In order to relate NO_2^- ion to total NO_2 a multiplication factor is necessary.

In work previously discussed, this equivalency factor ranges from 99 to 1.0 over the respective concentration ranges of 1 ppm to 1000 ppm. According to Brattan and Marshall, (1) and confirmed by Patty and Petty, (2) a good value for the concentration range under consideration (100-300 ppm) is 1.7 moles NO_2 per moles NO_2^- ion. Therefore, this equivalency factor was utilized.

1. Brattan and Marshall, J. Bio. Chem., 128, 537. (1939).

2. Patty and Petty, J. Ind. Hyg., 25, 361, (1943).

The Henry's law saturation values were taken from Figure C-1 for 100 and 300 ppm. The units were converted to (ug/ml) and the 1.7 factor was used to obtain the values cited previously as 1.51 ug NO_2^-/ ml and 4.51 ug NO_2^-/ ml.

The enhanced absorption discussed in the results section is devised by taking the total amount of absorption observed during optimum conditions, i.e., SSR=2.5, time of exposure = 15 secs., which for 300 ppm and 100 ppm were 6.87 and 3.05 ug NO_2^-/ ml respectively, and taking the difference between observed and expected, divided by expected.

Therefore, for 300 ppm:

$$\frac{6.87 - 4.51}{4.51} = 0.523 \text{ or } 52.3\%$$

for 100 ppm:

$$\frac{3.05 - 1.51}{1.51} = 1.020 \text{ or } 102\%$$

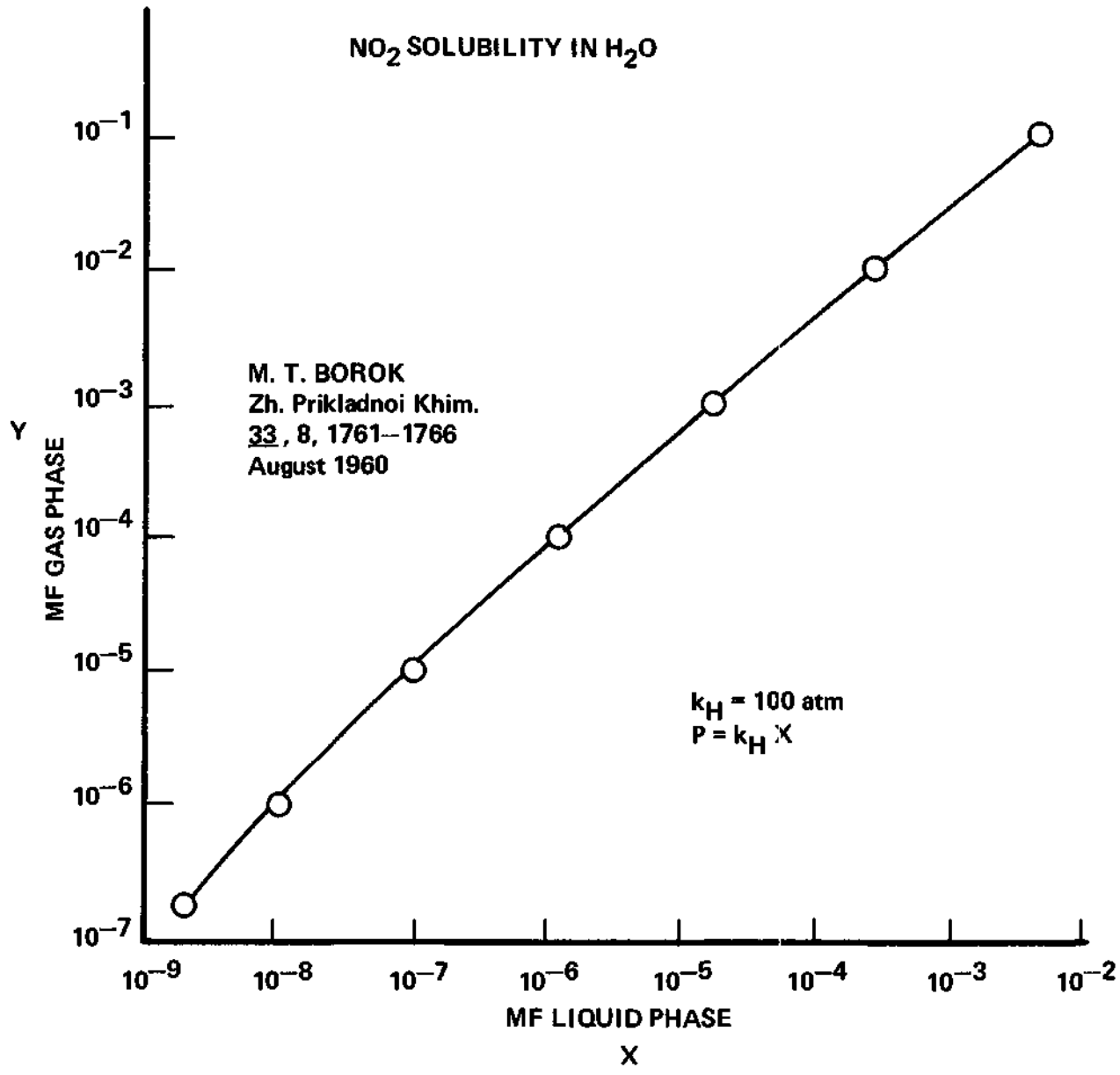

Figure C-1. Henry's Law Constant From Borok

APPENDIX D

CALIBRATION CURVES AND TESTING PROCEDURE USED

The experimental procedure employed in this experiment is a combination of the Saltzman method and ASTM 1607-69 which have been referenced in the Appendix. Slight modifications were made, as these procedures refer to air sampling rather than water sampling. Therefore, the experimental procedure followed in this experiment follows:

Reagents

N-(Naphthyl) - ethylenediamine Dihydrochloride (0.1%): Dissolve 0.1 gm of the reagent in 100 ml of H_2O.

Absorbing Reagent: Dissolve 5 gm sulfanilic acid in almost a liter of water containing 140 ml acetic acid, add 20 ml of the 0.1% stock solution of N-1(Naphthyl)-ethylenediamine Dihydrochloride, and dilute to 1 liter.

Standard Sodium Nitrate ($NaNO_2$) solution (0.0203 gm/l): One millileter of this working solution produces a color equivalent to 10µl of NO_2 in air. Prepare from Merck reagent grade granular solid, assayed at 99.4% dissolved in water to the desired wt %.

Procedure

1. It was originally thought that nitrite-free water, prepared by the method discussed in Standard Methods pp. 241 was necessary. However, the low ph of this solution necessitated its abandonment and, therefore, distilled, dionized water was used. No detectable NO_2^- was found in this water.

2. The standardization procedure used for the experiment follows: Graduated amounts of $NaNO_2$ solution up to 1 ml, measured accurately in a graduated pipet, were added to a series of 25 ml flasks containing 10 ml of the absorbing reagent. Fifteen minutes were allowed for color development. Enough samples of the standard solution were taken so that the experimental absorbance range could be observed. Absorbance was plotted against concentration and Beer's law was found to be valid in the concentration range.

3. The procedure for experimentally collecting the drops consisted of capturing the drops in a 25 ml flask containing 10 ml of the absorbing reagent. The absorbing agent acts as fixing agent, in that the consequent color development is the result of an ayo dye formation, i.e., diazosulfanilic acid.

The Calibration Curves used in the experiment are attached. Figure D-1 shows the rotatometer calibration curves. Figure D-2 shows the calibration curve for the thermister. Figure D-3 shows the calibration curve for the absorbance - concentration for the standard, $NaNO_2$, dissolved in the absorbing reagent. The experimental method is discussed here.

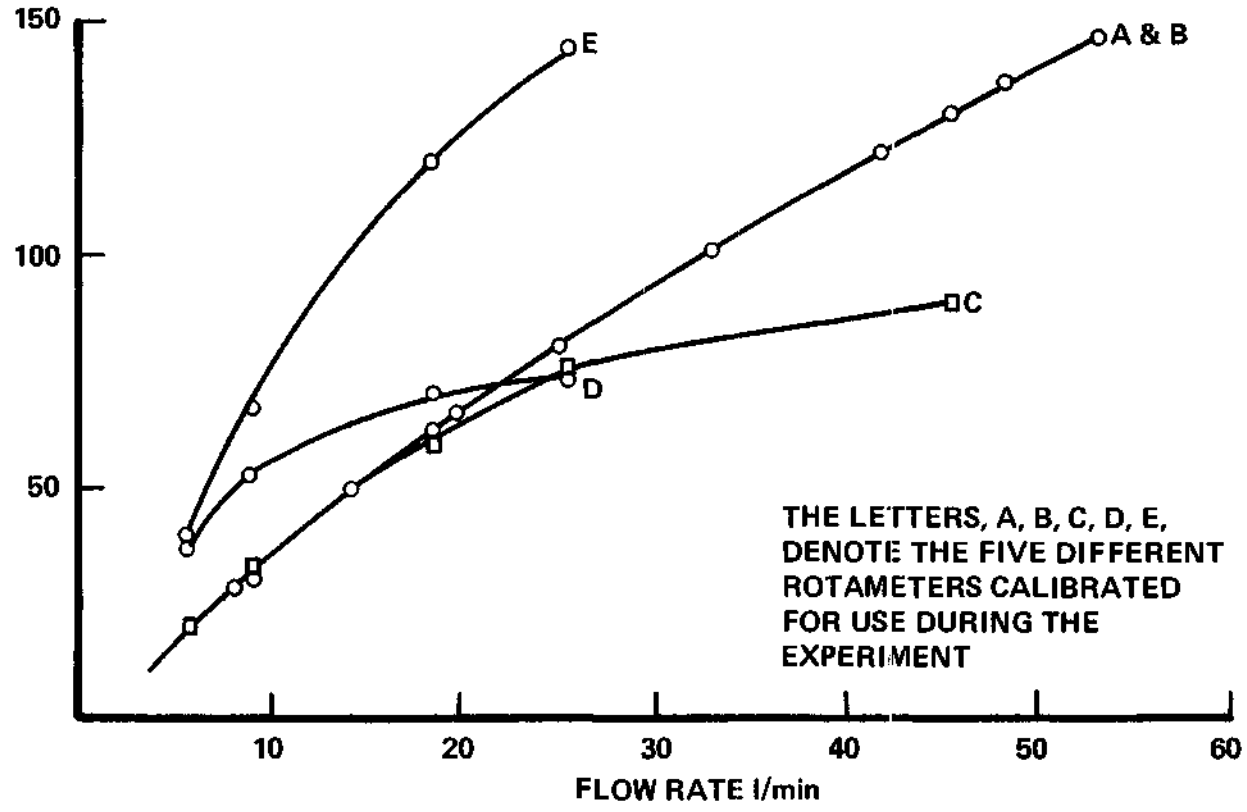

Figure D-1. Rotameter Calibration Curves

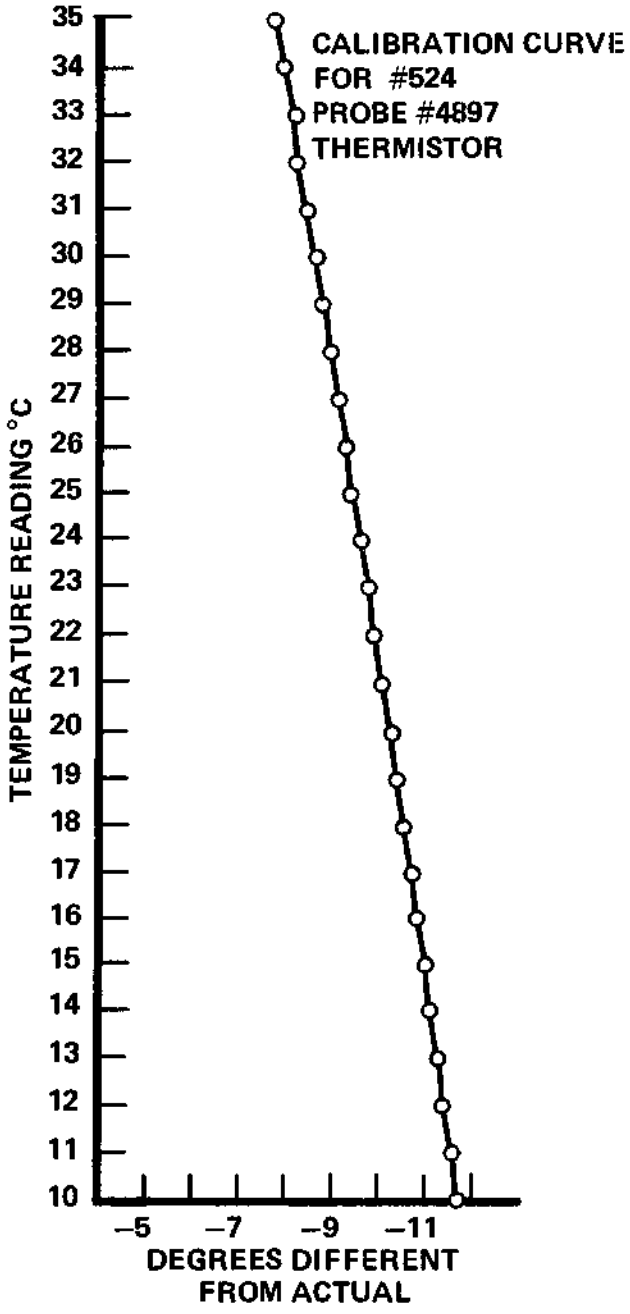

Figure D-2. Thermistor Calibration Curve

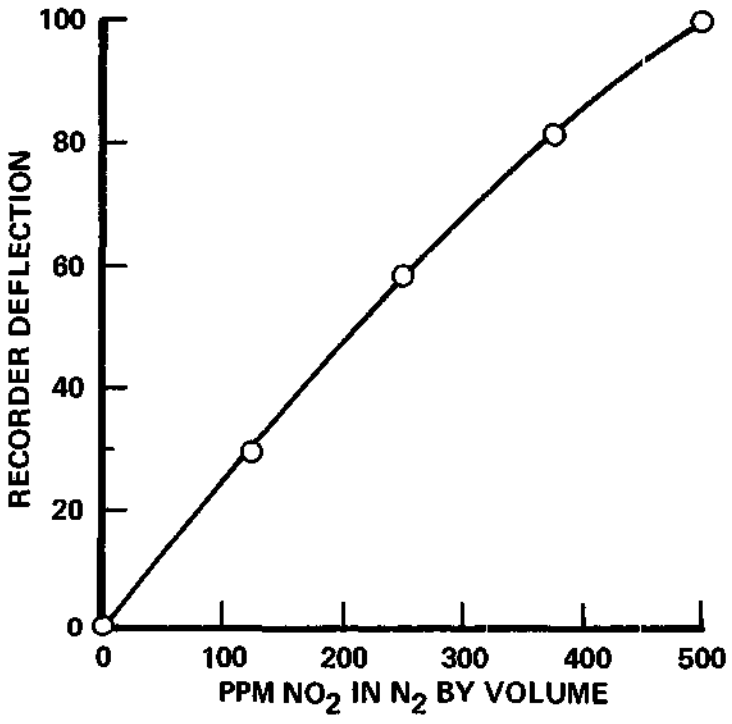

Figure D-3. UV Analyzer Calibration Curve

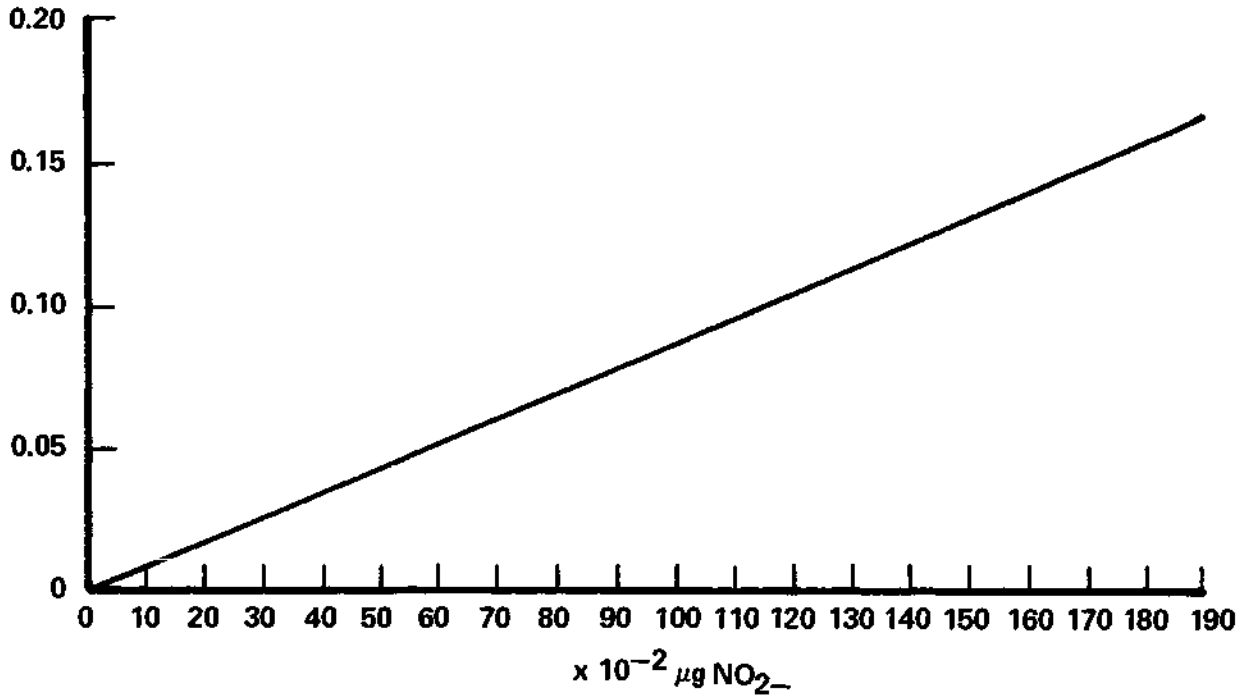

Figure D-4. Spectrophotometer Calibration Curve

APPENDIX E

EXPERIMENTAL DATA AND CALCULATED RESULTS

Table E-1. Tabulated Results; Laboratory Results for 300 ppm Test

SSR	Time (Sec)	Absorbance
2.5	5	0.027
		0.028
		0.027
	10	0.029
		0.028
		0.028
	15	0.033
		0.033
		0.033
	20	0.032
		0.033
		0.032
	25	0.022
		0.022
		0.021
	30	0.021
		0.022
		0.022
	60	0.021
		0.022
		0.022

Table E-1. Continued

SSR	Time (Sec)	Absorbance
2.0	5	0.026
		0.025
		0.026
	10	0.027
		0.027
		0.026
	15	0.026
		0.026
		0.025
	20	0.024
		0.023
		0.024
	25	0.022
		0.022
		0.021
	30	0.021
		0.021
		0.021
	60	0.021
		0.022
		0.022

Table E-1. Continued

SSR	Time (Sec)	Absorbance
1.5	5	0.024
		0.023
		0.023
	10	0.023
		0.022
		0.023
	15	0.022
		0.021
		0.023
	20	0.021
		0.021
		0.020
	30	0.021
		0.021
		0.021
	60	0.020
		0.020
		0.021

Table E-1. Continued

SSR	Time (Sec)	Absorbance
1.0	5	0.024
		0.023
		0.024
	10	0.023
		0.023
		0.023
	15	0.022
		0.022
		0.022
	20	0.020
		0.020
		0.020
	30	0.020
		0.019
		0.019
	60	0.019
		0.019
		0.019

Table E-2. Tabulated Results; Laboratory Results for 100 ppm Test

SSR	Time (Sec)	Absorbance
2.5	5	0.014
		0.014
		0.014
	10	0.014
		0.013
		0.016
	15	0.015
		0.014
		0.015
	20	0.010
		0.009
		0.008
	30	0.007
		0.007
		0.007
	60	0.007
		0.007
		0.007

Table E-2. Continued

SSR	Time (Sec)	Absorbance
2.0	5	0.012
		0.012
		0.012
	10	0.012
		0.012
		0.012
	15	0.012
		0.011
		0.012
	20	0.008
		0.008
		0.008
	30	0.007
		0.007
		0.007
	60	0.006
		0.007
		0.007

Table E-2. Continued

SSR	Time (Sec)	Absorbance
1.5	5	0.009
		0.010
		0.010
	10	0.009
		0.009
		0.010
	15	0.008
		0.008
		0.008
	20	0.007
		0.008
		0.008
	30	0.007
		0.007
		0.007
	60	0.007
		0.006
		0.007

Table E-2. Continued

SSR	Time (Sec)	Absorbance
1.0	5	0.007
		0.008
		0.008
	10	0.009
		0.007
		0.008
	15	0.008
		0.008
		0.008
	20	0.007
		0.007
		0.007
	30	0.007
		0.006
		0.007
	60	0.006
		0.006
		0.007

Table E-3. Tabulated Results; Calculated Results for 300 ppm Test

SSR	Time (Sec)	Concentration (ug/ml) NO_2^-
2.5	5	5.75
	10	5.95
	15	6.87
	20	6.71
	25	4.50
	30	4.50
	60	4.50
2.0	5	5.38
	10	5.52
	15	5.40
	20	4.90
	25	4.50
	30	4.40
	60	4.50
1.5	5	5.20
	10	5.00
	15	4.79
	20	4.50
	25	
	30	4.58
	60	4.60
1.0	5	5.05
	10	4.95
	15	4.79
	20	4.35
	30	4.35
	60	4.35

Table E-4. Tabulated Results; Calculated Results for 100 ppm Test

SSR	Time (Sec)	Concentration (ug/ml) NO_2^-
2.5	5	2.90
	10	3.02
	15	3.05
	20	2.00
	30	1.50
	60	1.45
2.0	5	2.50
	10	2.50
	15	2.45
	20	1.67
	30	1.45
	60	1.40
1.5	5	2.07
	10	1.98
	15	1.72
	20	1.69
	30	1.50
	60	1.50
1.0	5	1.61
	10	1.72
	15	1.72
	20	1.50
	30	1.50
	60	1.50

APPENDIX F

ABSORPTION VERSUS CONDENSATION

In Figure 11, an attempt was made to relate absorption against condensation by removing the mechanism of ordinary absorption at a particular time. This was done by taking the amount absorbed at a particular time when absorption was known to occur, i.e., at 5 and 10 seconds for SSR 2.5 and 2.0, and by taking the difference in the amount absorbed and comparing this to the amount of water condensed associated with this difference.

The points shown on Figure 11 indicate that a very limited amount of data was available since condensation occurred for such a short period.

Table F-1. Results Showing Amount Absorbed and Amount Condensed

Condensed H_2O vs. Moles Absorbed NO_2			
ppm	Time(Sec)	Amount Condensed (mo H_2O)	Amount Absorbed (mo NO_2)
300	5	.4571 - .4561 = .001	2.10 - 1.96 = .14
300	10	.4592 - .4576 = .0016	2.28 - 2.02 = .26
100	5	.001	1.06 - .92 = .14
100	10	.0016	1.10 .92 = .16

ppm	Slopes Calculated
300	$\frac{1.05 - .98}{.0036 - .0026} = \frac{70 \text{ Moles } NO_2 \text{ absorbed}}{\text{Moles } H_2O \text{ absorbed}}$
100	$\frac{1.09 - .98}{.0057 - .0026} = \frac{.11}{.0031} = \frac{35.48 \text{ Moles } NO_2}{\text{Moles } N_2O}$

BIBLIOGRAPHY

1. American Public Health Assoc., Standard Methods for Examination of Water and Wastewater; Nitrite, 13th Ed., 240 (1971).

2. Angelo, J. B., Lightfoot, E. N., and Howard, D. W., "Generalization of the Penetration Theory for Surface Stretch: Application to Forming Oscillating Drops", J. Am. Inst. Chem. Engr., 12(4), 751. (1966).

3. Bagaevskii, O. A., "Adsorption of a Gas on a Growing Drop", Zh. Fiz. Khim., 43, 1298. (1969).

4. Becker, H. G., "Mechanism of Absorption of Moderately Soluble Gases in Water", Ind. Eng. Chem., 16, 1220. (1924).

5. Bird, R. B., Stewart, W. G., and Lightfoot, E. N., Transport Phenomena, John Wiley and Sons, Inc., New York, 1974.

6. Borok, M. T., "Dependence of the Degree of Absorption of Nitrogen Dioxide in Water on its Concentration in a Gaseous Mixture", Zh. Prik. Khim., 33, 8, 1761. (1960).

7. Caudle, P. G. and Denbigh, K. G., "Chemical Reaction in the Liquid Phase of N_2O_4 and Water", Trans Faraday Soc., 49, 39. (1953).

8. Caudle, P. G. and Denbigh, S. S., "The Mechanism of Liquid - Liquid Extraction Across Stationary and Moving Interfaces -- I. Mass Transfer Into Single Dispensed Drops", Chem. Eng. Sci., 1(5), 197. (1952).

9. Crecelius, H., and Forwerg, W., "Investigations of the Saltzman Factor", Staub - Reinhalt Luft 30, 7, 23. (1970).

10. Danckwerts, P. U., "Significance of Liquid - Film Coefficient in Gas Absorption", Ind. Eng. Chem., 43(6), 1460.

11. Dekker, W. A., Snoeck, E. and Kramers, H., "The Rate of Absorption of NO_2 in Water", Chem. Eng. Sci., 11, 61. (1959).

12. Denbigh, K. G. and Prince, A.J., "Absorption of N_2O_4 in Water", J. Chem. Soc., 790, (1947).

13. Dixon, B. E., and Russell, A. W., "The Absorption of CO_2 by Liquid Drops", J. Soc. Chem. Ind., 69, 284. (1950).

BIBLIOGRAPHY (Continued)

14. England, E. and Corcoran, W. H., "The Rate and Mechanism of The Air Oxidation of Parts - per - Million Concentrations of Nitric Oxide in the Presence of Water Vapor", Ind. Eng. Chem. Fund., 14, 1, 55. (1975).

15. Fuks, N. A., Evaporation and Droplet Growth in Gaseous Media, Pergammon Press, New York, 1959.

16. Giardina, P. J. and Matteson, M. J., "Mass Transfer of SO_2 to Growing Droplets: Role of Surface Electrical Properties" Env. Sci. Tech., 8, 50. (1974).

17. Gilliland, E. R., and Hughes, P. R., "Mass Transfer Inside Drops in a Gas", Chem. Eng. Prog. Symp. Series, 51(16), 101. (1955).

18. Griess - Saltzman Method, ASTM, D1607-69, 498. (1976).

19. Griffith, P. M., "Mass Transfer from Drops and Bubbles", Chem. Eng. Sci., 12, 198. (1960).

20. Groothius, H. and Kramers, H., "Gas Absorption by Single Drops During Formation", Chem. Eng. Sci., 4, 17. (1955).

21. Higbie, R., "The Rate of Absorption of a Pure Gas Into a Still Liquid During Short Periods of Exposure", Trans. Am. Inst. Chem. Engr., 31, 365. (1935).

22. Johnstone, H. F., and Williams, G. C., "Absorption of Gases by Liquid Droplets", Ind. Eng. Chem., 31, 993, (1939).

23. Jones, G., and Ray, W. H., "The Surface Tension of Solutions of Electrolytes as a Function of Concentration", J. Am. Inst. Chem. Engr., 10, 5, 6711 (1964).

24. Jones, K., "Nitrogen Dioxide and Dinitrogen Tetroxide". Comprehensive Inorganic Chemicals, Vol. II. Pergammon Press, New York. pp. 340, 1973.

25. Kameoka, Y. and Pigford, R. L., "Absorption of Nitrogen Dioxide Into Water, Sulfuric Acid, Sodium Hydroxide, and Alkaline Sulfite Agueous Solutions". Ind. Eng. Chem. Fund., 16, 1, 163. (1977).

26. Kramers, H. and Beek, W. J., "Mass Transfer with a Change in Interfacial Area", Chem. Ing. Sci., 16, 909. (1962).

27. Kramers, H. and Lynn, S., "Absorption Studies in the Light of the Penetration Theory -- III. Absorption by Wetted Spheres, Singly and in Columns", Chem. Eng. Sci., 4(2), 63. (1955).

BIBLIOGRAPHY (Continued)

28. Kuo, C. H., and Huang, C. J., "Simultaneous Gas Absorption and Consecutive Reversible Chemical Reactions", Chem. Eng. J., 5, 43,

29. Lewis, W. K., and Whitman, W. G., "Principles of Gas Absorption", Ind. Eng. Chem., 16, 1215. (1924).

30. Mellor, M., Treatise on Inorganic and Theoretical Chemistry, Vol. VIII, pp. 258, 1960.

31. Oliver, M. J., "The Absorption of Oxygen by Water Droplets During Condensation", M. S. Thegis, Georgia Institute of Technology, 1976.

32. Palmers, E. D., Gunnisan, A. F., Dimattio, J., and Tomczyk, C., "Personal Sampler for Nigrogen Dioxide", Am. Ind. Hyg. Assoc. J., 37, 570. (1976).

33. Perry, J. H., Ed., Chemical Engineers' Handbook, Fourth Edition, McGraw-Hill Book Co., New York, pp. 14-37, 1950.

34. Peters, M. S., Ross, C. P., and Klin, J. E., "Controlling Mechanism in the Agueous Absorption of Nitrogen Oxides". AICHE J. 1, 105. (1955).

35. Popovich, A. T., "Mass Transfer During Single Drop Formation", Chem. Eng. Sci., 19, 351. (1964).

36. Prausnitz, J. M., Molecular Thermadynamics of Fluid Phase Equilibrium, Prentice-Hall, Inc., Englewood Cliffs, N.J. (1969).

37. Rajan, S. M., and Hiedeger, W. J., "Drop Formation Mass Transfer", J. Am. Inst. Chem. Engr., 17(1), 202. (1971).

38. Saltzman, B. E., "Colorimetric Microdetermination of Nitrogen Dioxide in the Atmosphere", Anal. Chem., 26, 1949. (1954).

39. Sawicki, E., Johnson, H. and Stanley, T. W., "Determination of Nitrate or Natrate plus Nitrite with 1 - Aminopyrene", Anal. Chem. 25, 12, 1934. (1963).

40. Sherwood, T. K. and Pigford, R. L., Absorption and Extraction, McGraw-Hill Book Co., New York, pp. 368-383. (1952).

41. Sherwood, T. K., Pigford, R. L. and Wilke, C. R., Mass Transfer, McGraw-Hill Book Co., New York. (1975).

42. Terovskaya, A. M., and Belopolskii, A. P., Zhur. Fiz. Khim., 24, 981. (1950).

43. Treyball, R. E., Mass Transfer Operations, Second Edition, McGraw-Hill Book Co., New York, 1955.

44. Whitman, W. G., and Davis, W. G., "Comparative Absorption Rates for Various Gases", Ind. Eng. Chem. 16, 1233. (1924)

45. Whitman, W. G., Long, L., and Wang, H. Y., "Absorption of Gases by a Liquid Drop", Ind. Eng. Chem., 18, 363. (1926).

46. Wills, T. L. "The Absorption of Sulfur Dioxide by Water Droplets During Condensation", M. S. Thesis, Georgia Institute of Technology, 1975.

47. Zhidkov, B. A. and Skvortsov, G. A., "Selection of Equilibrium Constant of Nitrogen Dioxide Reaction with Water", Sov. Chem. Ind., 11, 747. (1971).